

Anomalous Fluctuations of Directed Polymers in Random Media

Terence Hwa* and Daniel S. Fisher

Lyman Laboratory of Physics, Harvard University, Cambridge, MA 02138

(May 8, 2018)

Abstract

A systematic analysis of large scale fluctuations in the low temperature pinned phase of a directed polymer in a random potential is described. These fluctuations come from rare regions with nearly degenerate “ground states”. The probability distribution of their sizes is found to have a power law tail. The rare regions in the tail dominate much of the physics. The analysis presented here takes advantage of the mapping to the noisy-Burgers’ equation. It complements a phenomenological description of glassy phases based on a scaling picture of droplet excitations and a recent variational approach with “broken replica symmetry”. It is argued that the power law distribution of large thermally active excitations is a consequence of the continuous statistical “tilt” symmetry of the directed polymer, the breaking of which gives rise to the large active excitations in a manner analogous to the appearance of Goldstone modes in pure systems with a broken continuous symmetry.

Typeset using REVTeX

I. INTRODUCTION

The statistical mechanics of directed polymers in random media has attracted much attention in recent years [1–5]. This problem and related problems of higher dimensional manifolds are encountered in a variety of contexts, ranging from the fluctuations of domain walls in random magnets [1,6,7], to the dynamics of magnetic flux lines in dirty superconductors [8,9]. In addition, the randomly-pinned directed polymer is one of the simplest models that contain many of the essential features of strongly frustrated random systems such as spin-glasses [10]. Understanding the behavior of the directed polymer is therefore important for developing intuition and testing theoretical ideas for more complicated random systems.

Over the years, a variety of methods have been used to study random directed polymers. These include mapping [2,3] to a hydrodynamic system: the noise-driven Burgers equation [11,12], the exact solution on a Cayley tree [13], Migdal-Kadanoff approximate renormalization group calculations [14], a Bethe ansatz solution in 1+1 dimensions using replicas [15,16], a gaussian variational ansatz in replica space [17], and finally, renormalization group arguments and phenomenology [18] in the spirit of the droplet (or scaling) theory of spin-glasses [19]. There have also been substantial numerical simulations; some recent studies can be found in Refs. [18,20–22]. The qualitative phase diagram of the directed polymer is found to be quite simple: There is always a pinned phase dominated by disorder at low temperatures. For polymers in $d + 1$ dimensions, only the pinned phase exists for $d \leq 2$. But for $d > 2$, the polymer can undergo a continuous transition to a high-temperature phase where the disorder is irrelevant as has been proved rigorously [23]. Until recently, most of the efforts have been focused on characterizing the scaling properties of the polymer displacements and free energy fluctuations in the pinned phase. With the exception of 1+1 dimensions for which the scaling exponents can be computed exactly, systematic and analytic computations of the exponents at the zero temperature fixed point that controls the pinned phase have not been possible so far.

Some of the other properties of the glassy pinned phase beyond the scaling exponents

were explored numerically by Zhang [24], and more recently by Mézard [20]. These authors find very sensitive dependence of the polymer's low temperature configuration on the details of the particular random medium. Such sensitivity is associated with rare but singular dependence on the details of the random potential of the system. This type of behavior, including sensitivity to small temperature changes, has been predicted by Fisher and Huse [18] by phenomenological scaling and renormalization group arguments. As argued in Ref. [18] (and supported by numerical simulations in [18,20,24]), the physics of the low temperature phase is dominated by large scale, low energy excitations of rare regions, analogous to the droplet excitations proposed for Ising spin glasses [19]. Although the picture developed there is physically appealing and relatively complete, the phenomenological approach of Ref. [18] does not provide a systematic or quantitative way of calculating the properties of the pinned phase. On the other hand, various uncontrolled approximations can provide quantitative information. In particular, the Migdal-Kadanoff calculations of Derrida and Griffiths [14] could be used to study the properties predicted in Ref. [18] although this has not been carried out in detail. Mézard and Parisi [17] have recently proposed a very different approach: a variational method in replica space which can be used to study various aspects of the pinned phase. However, the method is limited by the gaussian Ansatz used whose physical significance is not clear, and the analysis based on replicas is haunted by the usual problem of the interchange of the $n \rightarrow 0$ and the thermodynamic limits. This is particularly problematic because within the gaussian Ansatz, one finds that the solution selected requires broken replica symmetry, the physical interpretation of which (if any) is unclear. (Note that the *correct* scaling exponents were obtained in 1+1 dimensions by using the Bethe Ansatz in replica space *without* breaking replica symmetry [15].)

In this paper, we explore the properties of the pinned phase of random directed polymers by using a more conventional approach based on a field-theoretic description without replicas, and the statistical symmetries of the problem. We will see that the *existence* of scaling forms for long wavelength, low frequency correlators of the noisy-Burgers' equation *implies*, without significant additional assumptions, the existence of rare large scale, low

energy “droplet” excitations with a power-law distribution of their sizes. Although the large thermally active excitations are very rare, they dominate many thermodynamic properties and average correlation and response functions, as well as causing large variations in the properties of macroscopic systems. We therefore see that many of the properties of the pinned phase predicted by Fisher and Huse [18] and found in other uncontrolled approximations can be recovered from the existence of a fixed point which, in the hydrodynamic language, is rather conventional. A fundamental lesson from this is that the broken continuous statistical symmetry of the pinned phase of the directed polymer gives rise, quite generally, to power law distribution of large rare, low energy excitations; these are the analog for broken continuous statistical symmetries of the Goldstone modes associated with true broken continuous symmetries !

This paper is presented in a somewhat pedagogical fashion. It is intended to introduce the ideas of rare fluctuations as well as providing an alternative perspective for those familiar with the scaling approach to directed polymers and spin glasses. The paper is organized as follows: In Section II, we define the directed polymer problem and some of the glassy properties of the pinned phase. We motivate the considerations of almost degenerate ground states that give rise to large scale, low energy excitations, and relate their statistics to the distribution functions of the end point of a polymer. The distribution functions are computed in Section III by using a free-energy functional (described in Appendices A and B) and by exploiting the statistical symmetries (Appendix C). The results are interpreted in terms of the large, rare fluctuations in the pinned phase, with a short discussion contained in Section IV. The results of this study are then compared with the variational approach of Ref. [17] and the phenomenological approach of Ref. [18]. We conclude that the various approaches point to the same physics governing the excitations of the directed polymer at low-temperatures — the physics of large, rare fluctuations.

II. PROPERTIES OF THE PINNED PHASE

A. The Model

We consider a directed polymer of length t (which will later be convenient to consider as “time”) embedded in $d + 1$ dimensions. Let the position vector $(\vec{\xi}(z), z)$ with $\vec{\xi} \in \mathfrak{R}^d$ and $0 \leq z \leq t$ describe the path of the polymer in the d transverse dimensions. Then the statistical mechanics of this polymer is determined by the Hamiltonian

$$\mathcal{H}[\vec{\xi}, \eta] = \int_0^t dz \left[\frac{\kappa}{2} \left(\frac{d\vec{\xi}}{dz} \right)^2 + \eta(\vec{\xi}(z), z) \right], \quad (2.1)$$

where κ is the line tension, and η is a quenched random potential of the medium through which the polymer passes. The random potential can be taken to be uncorrelated and gaussian distributed, with $\bar{\eta} = 0$ and

$$\overline{\eta(\vec{x}, z)\eta(\vec{x}', z')} = 2D\delta^d(\vec{x} - \vec{x}')\delta(z - z'). \quad (2.2)$$

Here, the overbar denotes averages over η , and D characterizes the strength of the random potential. Note that a cutoff on the spatial delta function is necessary for $d \geq 2$.

In order to make our subsequent discussions precise, it is useful to fix one end of the polymer at an arbitrary point, say at $\vec{\xi}(t) = \vec{x}$. This is implemented by introducing the one-point restricted partition function,

$$Z(\vec{x}, t) = \int \mathcal{D}[\vec{\xi}] \delta^d(\vec{\xi}(t) - \vec{x}) e^{-\mathcal{H}[\vec{\xi}, \eta]/T}, \quad (2.3)$$

where the arguments of Z give the coordinate of the fixed end point. Unless otherwise indicated, thermal averages will be performed using this restricted partition function, and will be denoted by $\langle \dots \rangle$.

The partition function $Z(\vec{x}, t)$ is, of course, a random variable because of its dependence on the realization of the random potential η . For a particular realization of η , the Hamiltonian has no symmetries. However, because of the translational invariance in both \vec{x} and t of the *statistics* of η , the *distribution* of \mathcal{H} has *statistical translational symmetry* in \vec{x} and

t . Thus the statistics of Z and other properties will also be translationally invariant. As we shall see, this symmetry and the closely related “tilt” symmetry — which corresponds to a weakly t -dependent translation in \vec{x} — have dramatic consequences.

One of the simplest way to characterize the configuration of the polymer is the one-point distribution function:

$$P_1(\vec{y}, t_0 | \vec{x}, t) \equiv \langle \delta^d(\vec{\xi}(t_0) - \vec{y}) \rangle. \quad (2.4)$$

This function is the conditional probability of finding the segment, $\vec{\xi}(t_0)$, of the polymer at position (\vec{y}, t_0) given that the fixed end is at (\vec{x}, t) . (We use “|” to separate the positions of the free|fixed positions of the polymer as in conditional probability.) In the absence of disorder, this distribution is easily calculated, yielding the usual random-walk result

$$G^{(0)}(\vec{x} - \vec{y}, t - t_0) \equiv P_1^{(0)}(\vec{y}, t_0 | \vec{x}, t) = \left(\frac{\kappa}{2\pi T(t - t_0)} \right)^{d/2} \exp \left[-\frac{\kappa}{2T} \frac{(\vec{x} - \vec{y})^2}{t - t_0} \right], \quad (2.5)$$

where the superscript (0) denotes the pure system with $D = 0$. The second moment of this distribution gives the mean transverse displacement,

$$\langle |\vec{X}(t - t_0)|^2 \rangle^{(0)} \equiv \langle |\vec{\xi}(t) - \vec{\xi}(t_0)|^2 \rangle^{(0)} \equiv \int d^d \vec{r} \vec{r}^2 G^{(0)}(\vec{r}, t - t_0) = \frac{Td}{\kappa} (t - t_0). \quad (2.6)$$

The existence of the random potential tends to increase the transverse wandering of the polymer, as it tries to take advantage of favorable regions of the random potential at low temperatures. After averaging over the disorder, translational symmetry in space is restored, and we have $\overline{P_1}(\vec{y}, t_0 | \vec{x}, t) = G_t(\vec{x} - \vec{y}, t - t_0)$. Note that a subscript t is used to indicate the explicit dependence of G on the polymer length; we have not put this subscript on P_1 since it already has the explicit t dependence. Numerically, it is found that

$$\overline{\langle |\vec{X}_t(\tau)|^2 \rangle} \equiv \int d^d \vec{r} \vec{r}^2 G_t(\vec{r}, \tau) = \tau^{2\zeta} f(\tau/t), \quad (2.7)$$

with $f(s)$ being a smooth scaling function which is finite throughout the range $0 \leq s \leq 1$, and the wandering (or roughness) exponent is $1/2 < \zeta < 3/4$ depending on the dimensionality d [25]. In 1+1 dimensions, the exponent $\zeta = 2/3$ has been obtained exactly by a number

of methods [2,15]. The power law dependence of the transverse displacement reflects the lack of intrinsic scales. This is possible because of the statistical translational symmetry, $\vec{\xi} \rightarrow \vec{\xi} + \text{const}$ of the Hamiltonian (2.1) as discussed above. In dimensions $d > 2$, there is a high temperature or weak randomness phase in which $\zeta = 1/2$, in addition to the low temperature pinned phase on which we shall focus. It has been conjectured [18] that $\zeta > 1/2$ for all finite d in the pinned phase although this is controversial.

The detailed form of the disorder-averaged end point function G_t is much harder to obtain than the scaling exponent, even numerically [21,22]. It is expected to have the general form

$$G_t(\vec{r}, \tau) \approx \tau^{-d\zeta} \tilde{g}_{t/\tau}(r/\tau^\zeta) \quad (2.8)$$

by simple scaling and normalization requirements, with the scaling function \tilde{g} depending only weakly on t/τ but decaying rapidly for $r \equiv |\vec{r}| \gg \tau^\zeta$. Two limits of particular interests are

$$G(\vec{r}, \tau) \equiv \lim_{t/\tau \rightarrow \infty} G_t(\vec{r}, \tau) \approx \tau^{-d\zeta} \tilde{g}_\infty(r/\tau^\zeta), \quad (2.9)$$

which describes the one-point distribution of a semi-infinite polymer, and

$$\tilde{G}(\vec{r}, t) \equiv G_t(\vec{r}, t) \approx t^{-d\zeta} \tilde{g}_1(r/t^\zeta), \quad (2.10)$$

which describes the distribution of position of the free end of a finite polymer. As explained in the Appendices, analytical studies of the problem is much simplified in the limit $t/\tau \rightarrow \infty$. For instance, $G(\vec{r}, \tau)$ is given to a good approximation by a self-consistent integral equation in 1+1 dimensions (See Appendix B and Ref. [26]). Numerical solution of the integral equation [26] yields the form Eq. (2.9), with $\tilde{g}_\infty(s)$ well approximated by a gaussian, although the precise shape of the tail is not known. However, in numerical simulations, it is most convenient to study the end-point distribution $\tilde{G}(\vec{r}, t)$. It is found [21,22] that the distribution function obeys the scaling form Eq. (2.10). A comparison between $\tilde{g}_\infty(s)$ and $\tilde{g}_1(s)$ shows that the scaling function at the two limits are quite similar: both are sharply decreasing functions whose widths are of order unity. Thus we see that the semi-infinite

polymer result $G(\vec{r}, \tau)$ gives the correct *scaling* behavior and the qualitative form of the scaling function for the end-point distribution of a finite polymer. We shall use this approximation in the following sections, where we will compute various distribution functions for a semi-infinite polymer (i.e., for $\tau \ll t$) and then apply them to the end point of a finite polymer with $\tau = t$.

B. Ground States

The description of the directed polymer given so far is rather conventional. The form of G_t in Eq. (2.8) describes a generic polymer. To appreciate the *glassy* nature of the pinned phase, it is necessary to go beyond the description in terms of the mean $\overline{P_1}$. We first note that an exponent $\zeta > 1/2$ in the pinned phase implies that the energy scales involved in the pinned phase are large. From the first term in (2.1), we see that a displacement of order t^ζ of the free end costs a minimum elastic energy of order $t^{2\zeta-1}$ which grows for long polymers. Growth of the characteristic energy scale for order parameter variation with length scale in conventional systems implies that the system is in an ordered phase governed by a zero temperature fixed point. Although there is no “order parameter” in the directed polymer, the displacement $\vec{\xi}(z)$ play a similar role and growth of the energy scale for variations of ξ with length scale — here t — implies that the pinned phase is controlled by a zero temperature renormalization group fixed point whose properties control the scaling of various quantities such as G_t in Eq. (2.8). By analogy with the ordered phase in conventional statistical mechanical systems, we expect that the large scale properties of the pinned phase can be described in terms of a “ground (or equilibrium) state” or “states”, and fluctuations about or between these “states”. Thus the configuration of the polymer selected by “thermal” averaging should be the equilibrium “state” that optimizes the total free energy for a given realization of the random potential. At zero temperature for a finite polymer with one point fixed at (\vec{x}, t) , there will be a unique preferred path (see Fig. 1(a)), $\vec{\xi}^*(z)$, which is the ground state, i.e., the state with the lowest energy. Here, the term “state” refers to an *optimal* path

starting from the fixed end at (\vec{x}, t) . A well-defined thermodynamic limit exists for the state of a semi-infinite polymer if the thermal mean position $\langle \vec{\xi}(z) \rangle$ and all other properties of the polymer at *fixed* finite z/t tend to a unique limit for a specific sample as $t \rightarrow \infty$. The conjecture that this holds for almost all samples was made and supported in Ref. [18]. The above definition of state only makes sense at $T = 0$ after providing short distance cutoffs a_ξ and a_τ in the $\vec{\xi}$ and z directions respectively. At small but finite temperatures, thermal fluctuations wash out the effect of disorder at short length scales, and the polymer does not “feel” the random potential until scales $a_\xi(T)$ and $a_\tau(T) \sim a_\xi^{1/2}(T)$ [18]. For example, we have in $d = 1$

$$a_\xi(T) = T^3/\kappa D. \quad (2.11)$$

We can then study the “states” of the polymer coarse-grained on the scales $a_\xi(T)$ and $a_\tau(T)$. A natural conjecture is that at finite temperature the equilibrium state is still unique. What does this mean? If the one-point distribution function, $P_1(\vec{y}, t_0 | \vec{x}, t)$ for a *typical* sample has the general behavior sketched in Fig. 1(b) (solid line), i.e., a sharply-peaked function of \vec{y} centered about some $\vec{y}^* = \vec{\xi}^*(t_0)$, with a width of order $a_\xi(T)$ for $\tau = t - t_0 \gg a_\tau(T)$, then this, together with similar behavior for all $0 \leq z \leq t$, implies that there is a well-defined “state” $\vec{\xi}^*(z)$ at long length scales at finite temperature. As we shall see, this simple picture is roughly correct but with subtle modifications of the meaning of “typical” which crucially affect the physics. Note that the equilibrium state is the minimum of the *coarse-grained* Hamiltonian which includes effects of the entropy of small scale fluctuations. Thus, in general, as shown in Ref. [18], the equilibrium states for different temperatures of the *same* sample will be very different on long length scales.

The peak in P_1 (solid line in Fig. 1(b)) should be located within a transverse distance τ^ζ of \vec{x} for most samples, since the disorder-average \overline{P}_1 , sketched as the dashed curve in Fig. 1(b), has the characteristic scale $|\vec{y} - \vec{x}| \sim \tau^\zeta$. The sharpness of P_1 for a typical sample can be revealed by probing disorder moments of P_1 for *different* end points. For instance, from the joint two-point correlation function,

$$Q_t(\vec{y}_1 - \vec{x}, \vec{y}_2 - \vec{x}, t - t_0) \equiv \overline{P_1(\vec{y}_1, t_0 | \vec{x}, t) P_1(\vec{y}_2, t_0 | \vec{x}, t)}, \quad (2.12)$$

we can obtain the mean square of the (thermally averaged) displacement,

$$\overline{\langle \vec{X}_t(\tau) \rangle^2} = \int d^d \vec{y}_1 d^d \vec{y}_2 (\vec{y}_1 - \vec{x}) \cdot (\vec{y}_2 - \vec{x}) Q_t(\vec{y}_1 - \vec{x}, \vec{y}_2 - \vec{x}, \tau), \quad (2.13)$$

which is expected to behave as

$$\overline{\langle \vec{X}_t(\tau) \rangle^2} \approx \tau^{2\zeta} f'(\tau/t), \quad (2.14)$$

just like $\overline{\langle |\vec{X}(t)|^2 \rangle}$ in Eq. (2.7) in the pinned phase of the directed polymer but with a different scaling function f' . From Eqs. (2.7) and (2.14), we obtain the mean square of the *thermal* fluctuations about $\langle \vec{\xi}(t) \rangle$,

$$\begin{aligned} \overline{C_T(\tau, t)} &\equiv \overline{\langle |\vec{\xi}(t - \tau) - \langle \vec{\xi}(t - \tau) \rangle|^2 \rangle} = \overline{\langle |\vec{X}_t(\tau)|^2 \rangle} - \overline{\langle \vec{X}_t(\tau) \rangle^2} \\ &= \frac{1}{2} \int d^d \vec{y}_1 d^d \vec{y}_2 |\vec{y}_1 - \vec{y}_2|^2 Q_t(\vec{y}_1 - \vec{x}, \vec{y}_2 - \vec{x}, \tau). \end{aligned} \quad (2.15)$$

One would hope that this quantity $\overline{C_T(\tau, t)}$ would characterize the typical width of the one point distribution P_1 (solid line of Fig. 1(b)). From the above discussion, the conjectured uniqueness of the equilibrium states at finite T would suggest that $[\overline{C_T(\tau, t)}]^{1/2}$ would be the diameter of the “tube” in which the polymer fluctuates, with $\overline{C_T(\tau, t)}$ not growing with τ or t . We shall see however, that in fact $\overline{C_T(\tau, t)} \sim \tau$ in both the pinned and the high temperature phases. How is this consistent with the existence of an equilibrium state of the problem in the pinned phase? It has been argued [18] that for *typical* samples (in fact in almost all samples for large τ) $C_T(\tau, t)$ is of order unity, but *rare* samples have sufficiently large $C_T(\tau, t)$ that they dominate the sample (or disorder) average. In this paper, we will see that this conclusion arises in a very natural way and can be characterized analytically by a power law tail in the distribution of various quantities that are related to $C_T(\tau, t)$.

In conventional critical phenomena, it is often sufficient to characterize a system by characterizing a few moments of the fluctuations. However, for many random systems, such averages do not give an adequate account of what actually goes on in a *typical* sample,

since some properties are not “self-averaging”. The pinned phase of the directed polymer exhibits exactly this type of behavior [18,20,24] and thus cannot be well characterized by the knowledge of a few moments. For instance, we shall see that a small fraction of samples have nearly degenerate ground “states”, $\vec{\xi}_a^*(z)$ and $\vec{\xi}_b^*(z)$, with segments (say the free ends $\vec{\xi}_a^*(0) = \vec{y}_a^*$ and $\vec{\xi}_b^*(0) = \vec{y}_b^*$) located far away (i.e., $|\vec{y}_a^* - \vec{y}_b^*| \gg a_\xi(T)$), as shown in Fig. 2(a). Such states would be manifested in P_1 as widely separated peaks (Fig. 2(b)) at low temperatures. The occurrence of such degenerate “states” may be rare. However, if they survive in the thermodynamic limit, with $|\vec{y}_a^* - \vec{y}_b^*| \rightarrow \infty$ as $t \rightarrow \infty$, then they can still have important physical consequences, because these are just the type of states that give rise to large scale fluctuations at low temperatures. Such almost degenerate states are the low dimensional analog of the “droplets” [18,19] conjectured to govern much of the low temperature properties of spin glasses. The investigation of these large fluctuations is the focal point of this study. We are particularly interested in obtaining the statistics of the almost degenerate states and understanding the effects of these states on physical observables. We shall give a detailed account of these effects in the following sections.

C. Distribution Functions

There are a number of ways one can characterize the rare fluctuations. To find the relative abundance of samples which behave as Figs. 1 and 2, we can, for example, consider the probability that P_1 has the structure shown in Fig. 2, with two peaks separated by a displacement $\Delta \equiv |\vec{\Delta}|$ at $z = t - \tau$, i.e., at a distance τ from the fixed end. It is useful to consider the larger peak to correspond to the optimal path and the other to correspond to an excitation with displacement $\vec{\Delta}$ away from the optimal path. For the second peak to have a reasonable amplitude, the excitation free energy must be of order T or less, i.e., it is a *thermally active excitation*, which is analogous to an active “droplet” introduced for spin glasses. The probability of an active droplet excitation of displacement $\vec{\Delta}$ at a distance τ from the fixed end is obtained from the distribution Q_t as [27]

$$W_t(\vec{\Delta}, \tau) = \int d^d \vec{y}_1 d^d \vec{y}_2 \delta^d(\vec{y}_1 - \vec{y}_2 - \vec{\Delta}) Q_t(\vec{y}_1 - \vec{x}, \vec{y}_2 - \vec{x}, \tau). \quad (2.16)$$

Like the one-point distribution function G_t discussed in Sec.II.A, it will be convenient to consider

$$W(\vec{\Delta}, \tau) = \lim_{t/\tau \rightarrow \infty} W_t(\vec{\Delta}, \tau) \quad (2.17)$$

which, for large τ , is the probability distribution of active droplets in the bulk of a semi-infinite polymer. Note that the somewhat different distribution of active droplets at the free end ($z = 0$)

$$\widetilde{W}(\vec{\Delta}, t) = W_t(\vec{\Delta}, t) \quad (2.18)$$

is however the most readily measurable quantity numerically.

In the absence of disorder, the “bare” distribution $W^{(0)}$ is just a gaussian,

$$W^{(0)}(\vec{\Delta}, \tau) = \left(\frac{\kappa}{4\pi T\tau} \right)^{d/2} e^{-\frac{\kappa}{4T\tau} \Delta^2} \quad (2.19)$$

since $Q_t^{(0)} = P_1^{(0)} \cdot P_1^{(0)}$ independent of t . [Note that $W_t(\vec{\Delta}, \tau)$ is the probability that the distribution P_1 has weight at two points separated by $\vec{\Delta}$. Only if the samples in which this occurs behave as in Fig. 2 will the interpretation of this as the probability of a well-defined active excitation really be useful. In the absence of randomness, this interpretation is clearly incorrect.] With disorder, Q_t becomes highly nontrivial, and it is not easy in general to compute even the first few moments of W_t . The large- Δ tail of the distribution, which governs the large scale fluctuations at low temperature, is difficult to obtain both analytically and numerically. In Section III, we introduce a free-energy functional which enables us to compute the asymptotic form of $W(\vec{\Delta}, \tau)$ explicitly. We will show that the tail of $W(\vec{\Delta}, \tau)$ [and hence also the tail of $\widetilde{W}(\vec{\Delta}, t)$ if we ignore the dependence on t/τ] has a power law form.

One of the physical consequences of the nearly degenerate ground states is the behavior of the mean square thermal fluctuations of a given segment of the polymer, $C_T(\tau, t) = \langle \Delta^2 \rangle / 2$, which has an average value

$$\overline{C}_T(\tau, t) = \frac{1}{2} \overline{\Delta^2} = \frac{1}{2} \int d^d \Delta \Delta^2 W_t(\vec{\Delta}, \tau). \quad (2.20)$$

This quantity is related to the susceptibility of the polymer to a tilt, i.e., the response to a term added to the Hamiltonian (2.1),

$$\mathcal{H}_{\vec{h}}[\vec{\xi}, \eta] = \mathcal{H}[\vec{\xi}, \eta] - \int_{t_0}^t dz \vec{h} \cdot \frac{d\vec{\xi}}{dz}. \quad (2.21)$$

Thermal fluctuations of $\vec{\xi}(t_0)$ at a distance $\tau = t - t_0$ from the fixed end are simply proportional to the linear response [28] of the polymer by the fluctuation-susceptibility relation,

$$\chi[\eta] \equiv \frac{\partial}{\partial h_i} \langle \xi_i(t) - \xi_i(t_0) \rangle_{\vec{h} \rightarrow 0} = \frac{1}{Td} C_T(t - t_0, t), \quad (2.22)$$

where ξ_i is a component of $\vec{\xi}$, and the subscript \vec{h} denotes thermal average taken with respect to the new partition function,

$$Z(\vec{x}, t; \vec{h}) = \int \mathcal{D}[\vec{\xi}] \delta^d(\vec{\xi}(t) - \vec{x}) e^{-\mathcal{H}_{\vec{h}}/T}. \quad (2.23)$$

Since the random potential η in the Hamiltonian (2.1) does not single out any preferred direction in the $(\vec{\xi}, z)$ space, a *statistical tilt symmetry* — related to the translational symmetry — exists which is recovered upon disorder average. As a result, one can prove straightforwardly that on average, the applied tilt \vec{h} merely shifts the mean position of the polymer at t_0 to $\overline{\langle \vec{\xi}(t_0) \rangle}_{\vec{h}}} = \vec{x} - \vec{h}\tau/\kappa$ (see Appendix C and Ref. [29]). The disorder-averaged susceptibility is thus just

$$\overline{\chi} = \frac{\tau}{\kappa} = \frac{1}{2Td} \overline{\Delta^2}, \quad (2.24)$$

which is *exactly* the same as the susceptibility of the pure system.

If the statistical properties of the ground states are complicated as illustrated in Figs. 1(a) and 2(a), then the mean susceptibility $\overline{\chi}$ does *not* provide an adequate characterization. On the one hand, a sample such as the one shown in Fig. 1(a) will contribute very little to the average susceptibility at low temperatures since it is locked in a unique state, separated from the lowest excited state by a free energy difference $\gg T$. On the other hand, a sample

corresponding to Fig. 2(a) has nearly degenerate states. Thermal fluctuations will thus cause large scale “hopping” of the polymer from one state to the other. Thus the latter samples can give large contributions to the average susceptibility even though they occur rarely. The relative abundance of such samples is given by the susceptibility distribution function,

$$D_t(\chi, \tau) = \overline{\delta(\chi - \chi[\eta])}. \quad (2.25)$$

A first principles calculation of D_t would require the knowledge of the full distribution of the function P_1 , or at least all of its correlations,

$$\overline{P_1(\vec{y}_1, t_0 | \vec{x}, t) \cdots P_1(\vec{y}_n, t_0 | \vec{x}, t)};$$

this will not be attempted here. To obtain the qualitative behavior, we will instead *assume* that a sample with an active droplet of size Δ has a susceptibility of order $\chi \sim \Delta^2/(2Td)$. This assumption obviously will not be very good if there are *many* almost degenerate states that contribute equally to the susceptibility, but it should be reasonable if large scale degenerate states occur only rarely, as we will demonstrate is the actual case. Using this approximation, the susceptibility distribution can be simply obtained from the droplet distribution as

$$D_t(\chi, \tau) = \int \frac{d^d \vec{\Delta}}{\Delta^2/(2Td)} W_t(\vec{\Delta}, \tau) u[\chi/(\Delta^2/2Td)], \quad (2.26)$$

where $u(s)$ is a sharply peaked scaling function whose precise shape depends on more knowledge of the distribution of P_1 .

D. Free Energy Variations

The functions $W_t(\vec{\Delta}, \tau)$ and $D_t(\chi, \tau)$ introduced above describe the distribution of the polymer’s *equilibrium* fluctuations and susceptibilities. But in reality (experimentally or numerically), equilibration of a glassy system is often very difficult [30]. The reason is that the nearly degenerate states that give rise to large scale, low energy droplet excitations are typically separated by large energy barriers, and therefore have extremely long relaxation

times. Knowledge of the distribution of the barriers is therefore crucial in understanding the *dynamic* properties of the glassy polymers.

The details of the dynamics at low temperatures is very complex and beyond the scope of this paper. However, one can get a bound of the free energy barriers *within* the equilibrium theory. To do so, let us consider the nearly degenerate states shown in Fig. 2(a). To probe the free energy “landscape” between \vec{y}_a^* and \vec{y}_b^* , we would like to know $F(\vec{x}, t; \vec{y}, 0)$, the free energy of a polymer $\vec{\xi}(z)$ with *both* ends fixed at $\vec{\xi}(t) = \vec{x}$ and $\vec{\xi}(0) = \vec{y}$, and then vary \vec{y} in between \vec{y}_a^* and \vec{y}_b^* (see Fig. 3). The maximum, F^* , of $F(\vec{x}, t; \vec{y}, 0)$ in this range of \vec{y} gives a *lower bound* of the free energy barrier to move the end $\vec{\xi}(0)$ from \vec{y}_a^* to \vec{y}_b^* , since the polymer must pass through all intermediate states with $\vec{y}_a^* < \vec{y} < \vec{y}_b^*$, i.e., in a range of width Δ . Note that this does not take into account the *additional* barriers the polymer may encounter at intermediate states (see Fig. 4). At this point, it is not clear whether or not the cumulative effects of such barriers will be much larger than $\delta F^* = F^* - F(\vec{x}, t; \vec{y}_a^*, 0)$.

Unfortunately, with two ends fixed, F is difficult to compute analytically. What *can* be obtained readily (see Appendices A and B) is the statistics of the free energy of a polymer of length t with only *one* end fixed, which is just

$$F(\vec{x}, t) = -T \log Z(\vec{x}, t). \quad (2.27)$$

As shown by the numerical studies of Kardar and Zhang [4], two polymers with end points fixed at a distance $\Delta \lesssim t^\zeta$ apart will merge a distance $\Delta^{1/\zeta}$ from the fixed ends and coincide for the rest of the way (see Fig. 5). Since the free energy difference between two polymers with different end point positions will only arise from the section over which they differ, we expect the typical free energy difference, $F(\vec{x}, t; \vec{y}, 0) - F(\vec{x}, t; \vec{y}_a^*, 0)$, of an intermediate state in Fig. 3 with $|\vec{y} - \vec{y}_a^*| \sim O(\Delta)$, to scale the same way as the difference $F(\vec{x} + \vec{\Delta}, t) - F(\vec{x}, t)$ for the two polymers in Fig. 5. The latter is characterized by the free energy correlation function

$$C_F(\vec{\Delta}, t) = \overline{[F(\vec{x} + \vec{\Delta}, t) - F(\vec{x}, t)]^2} \quad (2.28)$$

which is conjectured to scale as

$$C_F(\vec{\Delta}, t) \sim \Delta^{2\alpha} \quad (2.29)$$

for $\Delta \ll t^\zeta$, with the exponent known to be *exactly* $\alpha = 1/2$ in 1+1 dimensions. Thus $\sqrt{C_F(\vec{\Delta}, t)}$ provides the lower bound for the barrier of formation of an intermediate active droplet, which is the typical scale for F^* .

On the other hand, two polymers with end points fixed at $\Delta \gg t^\zeta$ will not overlap at all and thus behave as if they are in independent samples. In this case,

$$C_F(\vec{\Delta}, t) \sim t^{2\theta} \quad (2.30)$$

with θ being the exponent characterizing the sample-to-sample free energy variations. A simple scaling form, which we shall see arises naturally, links the two limits:

$$C_F(\vec{\Delta}, t) = \Delta^{2\alpha} \tilde{c}(\Delta/t^\zeta) \quad (2.31)$$

yielding the scaling relation

$$\alpha = \theta/\zeta. \quad (2.32)$$

We will later derive the scaling law

$$\theta = 2\zeta - 1 \quad (2.33)$$

which arises simply from the naive contribution to the free energy from the elastic part of the Hamiltonian with displacement of order t^ζ .

III. STATISTICS OF RARE FLUCTUATIONS

In Section II, we defined a number of distribution functions and disorder averaged correlations functions which are useful in probing the glassy nature of the randomly-pinned directed polymer. To obtain these functions in a systematic way, and to uncover the interconnections among them, we shall use field theoretic methods. The disorder average will be replaced by an average over a weighting functional, which describes the probability distribution of the free energy. This method is inspired by the Martin-Siggia-Rose dynamic field theory [31] developed in the context of stochastic dynamics onto which the directed polymer can be mapped [2,3]. The explicit mapping to the noisy-Burgers equation is derived in Appendix B. Note however, that the method may not be limited to the directed polymer and is described in Appendix A for an arbitrary dimensional manifold for which the mapping to stochastic dynamics cannot be performed. In this section, we shall use this field theoretic method to obtain the tails of the distribution functions introduced in Section II.C. We shall limit our discussions to the semi-infinite polymer ($t \rightarrow \infty$) problem for which the analysis is the simplest. We then interpret the results to characterize the statistics of the large rare fluctuations.

A. Derivation of the Distribution Functions

1. Formalism

To obtain the tails of the distribution functions $W_t(\vec{\Delta}, \tau)$ and $D_t(\chi, \tau)$ defined in Section II.C, we need (see Eq. (2.16)) the disorder-averaged function $Q_t(\vec{y}_1 - \vec{x}, \vec{y}_2 - \vec{x}, \tau)$ defined in Eq. (2.12). As shown in Appendix A, various distribution functions can be generated by adding a source term to the Hamiltonian, e.g.,

$$\mathcal{H} \rightarrow \mathcal{H} + \int_0^t dz \tilde{J}(\vec{\xi}(z), z), \quad (3.1)$$

and then differentiating the corresponding average free energy, $\bar{F}(\vec{x}, t; \tilde{J})$ with respect to \tilde{J} . The resulting expressions are simple for the semi-infinite polymer. For instance,

$$\frac{\delta \bar{F}(\vec{x}, t; \tilde{J})}{\delta \tilde{J}(\vec{y}, t_0)} = \bar{P}_1(\vec{y}, t_0 | \vec{x}, t) = G(\vec{x} - \vec{y}, t - t_0), \quad (3.2)$$

and

$$\begin{aligned} G_{2,1}(\vec{x} - \vec{y}_1, \vec{x} - \vec{y}_2, t - t_0) &\equiv \frac{\delta^2 \bar{F}(\vec{x}, t; \tilde{J})}{\delta \tilde{J}(\vec{y}_1, t_0) \delta \tilde{J}(\vec{y}_2, t_0)} \\ &= -\frac{1}{T} \left[\overline{\langle \delta^d(\vec{\xi}(t_0) - \vec{y}_1) \delta^d(\vec{\xi}(t_0) - \vec{y}_2) \rangle} - Q(\vec{y}_1 - \vec{x}, \vec{y}_2 - \vec{x}, t - t_0) \right] \end{aligned} \quad (3.3)$$

In terms of the noisy-Burgers equation, the limit $t \rightarrow \infty$ corresponds to the statistical steady state, and G and $G_{2,1}$ are the linear and nonlinear response functions respectively (see Appendix B). It is instructive to consider the meaning of $G_{2,1}$ in the limit of zero temperature (with an appropriate short distance cutoff on the random potential): $G_{2,1}(\vec{x} - \vec{y}_1, \vec{x} - \vec{y}_2, \tau)$ is the limit of small ϵ of $1/\epsilon$ times the probability that the optimal paths passing through \vec{y}_1 and \vec{y}_2 a distance τ from the fixed end at (\vec{x}, t) both have energy within ϵ of the ground state. Since triple degeneracies are unlikely, this is non-zero when the ground state is doubly degenerate and $G_{2,1}$ is the “density of states” of degeneracies. In terms of $G_{2,1}$, the droplet distribution is

$$W(\vec{\Delta}, \tau) = \delta^d(\vec{\Delta}) + W'(\vec{\Delta}, \tau), \quad (3.4)$$

with

$$W'(\vec{\Delta}, \tau) = T \int d^d \vec{y}_1 d^d \vec{y}_2 \delta^d(\vec{y}_1 - \vec{y}_2 - \vec{\Delta}) G_{2,1}(\vec{x} - \vec{y}_1, \vec{x} - \vec{y}_2, \tau). \quad (3.5)$$

The free-energy functional described in Appendix A allows us to express higher-order distribution functions such as $G_{2,1}$ in terms of the one-point function G (see Eq. (A16)). For the directed polymer, the relevant result is

$$\begin{aligned} G_{2,1}(\vec{x} - \vec{y}_1, \vec{x} - \vec{y}_2, t - t_0) &= - \int d^d \vec{x}' d^d \vec{y}_1' d^d \vec{y}_2' dt' dt_1 dt_2 G(\vec{x} - \vec{x}', \tau - t') \\ &\Gamma_{1,2}(\vec{x}' - \vec{y}_1', t' - t_1; \vec{x}' - \vec{y}_2', t' - t_2) G(\vec{y}_1 - \vec{y}_1', t_1 - t_0) G(\vec{y}_2 - \vec{y}_2', t_2 - t_0), \end{aligned} \quad (3.6)$$

where $\Gamma_{1,2}$ is a “vertex function” which is natural in the context of the noisy-Burgers equation; it will be specified shortly. The expression can be represented diagrammatically as

in Fig. 6. We see that the joint distribution $G_{2,1}$ has been conveniently broken up as a convolution of a number of one-body distribution functions (the G 's), with the branching process controlled by the vertex $\Gamma_{1,2}$.

For a (statistically) translationally invariant system, it is convenient (after disorder averaging) to work in Fourier space, with

$$\widehat{G}(\vec{q}, \tau) = \int d^d \vec{r} G(\vec{r}, \tau) e^{i\vec{q} \cdot \vec{r}}. \quad (3.7)$$

The Fourier transform, \widehat{W}' , of W' in Eq. (3.5) becomes

$$\begin{aligned} \widehat{W}'(q, t - t_0) &= -T \int_0^t dt' \int_{t_0}^{t'} dt_1 \int_{t_0}^{t_1} dt_2 \widehat{G}(0, t - t') \\ &\quad \widehat{\Gamma}_{1,2}(\vec{q}, t' - t_1; -\vec{q}, t' - t_2) \widehat{G}(\vec{q}, t_1 - t_0) \widehat{G}(-\vec{q}, t_2 - t_0), \end{aligned} \quad (3.8)$$

where $\widehat{\Gamma}_{1,2}$ is the Fourier transform of the vertex function $\Gamma_{1,2}$. From the scaling form (2.9) for G , we have

$$\widehat{G}(\vec{q}, \tau) \approx \widehat{g}(q\tau^\zeta), \quad (3.9)$$

where $q = |\vec{q}|$. Also, $\widehat{G}(0, t) = 1$ by normalization of the probability distribution P_1 . Therefore we have the simple expression

$$\widehat{W}'(q, \tau) = -T \int_{-\infty}^{\tau} d\tau' \int_0^{\tau'} d\tau_1 \int_0^{\tau_1} d\tau_2 \widehat{\Gamma}_{1,2}(\vec{q}, \tau' - \tau_1; -\vec{q}, \tau' - \tau_2) \widehat{g}(q\tau_1^\zeta) \widehat{g}(q\tau_2^\zeta). \quad (3.10)$$

To proceed further, we need to know something about the vertex $\widehat{\Gamma}_{1,2}$. We are especially interested in the small q behavior since that is what will control the *tail* of the distribution $W(\vec{\Delta}, \tau)$. Note that the normalization of W requires that $\widehat{W}'(q \rightarrow 0, \tau) \rightarrow 0$, hence we must have $\widehat{\Gamma}_{1,2}(q \rightarrow 0) \rightarrow 0$ since $\widehat{g}(0) = 1$. Also, we recall that the mean susceptibility is $\bar{\chi} = \tau/\kappa$ due to the statistical tilt symmetry (Appendix C), and $\bar{\chi} = \frac{1}{2Td} \overline{\Delta^2}$ from the fluctuation-susceptibility relation (2.24). Thus,

$$\lim_{\tau \rightarrow \infty} \lim_{q \rightarrow 0} -\vec{\nabla}_{\vec{q}}^2 \widehat{W}'(q, \tau) = \frac{1}{d} \overline{\Delta^2} = \frac{2T}{\kappa} \tau. \quad (3.11)$$

Since $\vec{\nabla}_{\vec{q}} \widehat{g} = 0$ by symmetry, we must have from Eq. (3.11)

$$\widehat{\Gamma}_{1,2}(\vec{q}, \tau' - \tau_1; -\vec{q}, \tau' - \tau_2) = \frac{1}{\kappa} q^2 \gamma(\vec{q}, \tau' - \tau_1; -\vec{q}, \tau' - \tau_2), \quad (3.12)$$

with

$$\lim_{q \rightarrow 0} \int_{-\infty}^{\tau} d\tau' \int_0^{\tau} d\tau_1 \int_0^{\tau} d\tau_2 \gamma(\vec{q}, \tau' - \tau_1; -\vec{q}, \tau' - \tau_2) = \tau. \quad (3.13)$$

The simplest form of $\widehat{\Gamma}_{1,2}$ satisfying Eq. (3.13) is

$$\widehat{\Gamma}_{1,2}^{(0)}(\vec{q}, \tau' - \tau_1; -\vec{q}, \tau' - \tau_2) = \frac{1}{\kappa} q^2 \delta(\tau' - \tau_1) \delta(\tau' - \tau_2). \quad (3.14)$$

This is actually the form of the “bare” vertex, i.e., it is the *exact* vertex in the absence of the random potential, as the bare distribution $W^{(0)}$ in Eq. (2.19) is readily recovered by substituting Eq. (3.14) in Eq. (3.10). In Appendix C, we use the statistical tilt symmetry to derive some Ward identities which ensure that the *scaling* behavior of the droplet distribution obtained from the full vertex $\widehat{\Gamma}_{1,2}$ will have the same *form* as that obtained by using the bare vertex $\widehat{\Gamma}_{1,2}^{(0)}$. Using Eq. (3.14) then, Eq. (3.10) becomes

$$\widehat{W}'(q, \tau) \approx -\frac{T}{\kappa} q^2 \int_0^{\tau} d\tau' [\widehat{g}(q(\tau')^\zeta)]^2 \approx -\frac{T}{\kappa} q^{2-\zeta^{-1}} \widehat{w}(q^{1/\zeta} \tau), \quad (3.15)$$

where $\widehat{w}(s)$ is a scaling function whose precise form depends on the actual forms of \widehat{g} and $\widehat{\Gamma}_{1,2}$ (see Appendix C), but whose limits are simple, i.e., $\widehat{w}(s \rightarrow \infty) = \text{const}$ and $\widehat{w}(s \rightarrow 0) \rightarrow s$.

2. Results

The Fourier transform of W itself, $\widehat{W} = 1 + \widehat{W}'$, has a power-law singularity (an inverted cusp) for small q in the limit $\tau \rightarrow \infty$ as long as $\zeta > 1/2$. The singularity is only cutoff by τ , with $\widehat{W} \approx 1 - (T/\kappa) q^2 \tau$ for $q < \tau^{-\zeta}$. Inverse Fourier transforming \widehat{W} , we obtain the final result

$$W(\vec{\Delta}, \tau) \approx \frac{1}{\Delta^{d+2-\zeta^{-1}}} \widetilde{w}(\Delta/\tau^\zeta) \quad \text{for} \quad \Delta \gg a_\xi(T), \quad (3.16)$$

with the scaling function $\widetilde{w}(s)$ having the form $\widetilde{w}(0) = \text{const}$ and \widetilde{w} rapidly decreasing for $s \gg 1$. This result suggests the following scaling form for the full distribution for a polymer of length t ,

$$W_t(\vec{\Delta}, \tau) = \frac{1}{\Delta^{d+2-\zeta^{-1}}} \tilde{w}_{t/\tau}(\Delta/\tau^\zeta), \quad (3.17)$$

with $\tilde{w} = \tilde{w}_\infty$. Assuming that W_t has a weak dependence on t/τ as in G_t , the above result leads to a power law distribution of active droplets at the free ends,

$$\tilde{W}(\vec{\Delta}, t) = \frac{1}{\Delta^{d+2-\zeta^{-1}}} \tilde{w}_1(\Delta/t^\zeta). \quad (3.18)$$

which is cut off only by the finite length of the polymer. A similar result is obtained for the tail of the susceptibility distribution. From Eqs. (2.26) and (3.17), we have,

$$D_t(\chi, \tau) \approx \frac{1}{\chi^{2-(2\zeta)^{-1}}} \tilde{d}_{t/\tau}(\chi/\tau^{2\zeta}) \quad \text{for} \quad \chi \gg a_\xi^2/Td, \quad (3.19)$$

with $\tilde{d}_{t/\tau}$ being another scaling function which is qualitatively similar to $\tilde{w}_{t/\tau}$.

Note that Eqs. (3.16) through (3.19) should only hold in the scaling limit $\Delta \gg a_\xi(T)$, where the one-point function has the scaling form (3.9). To understand the form of crossover of $W(\vec{\Delta}, t)$ from $\Delta < a_\xi$ to $\Delta > a_\xi$, it is useful to consider the following approximate form of the one-point function,

$$\hat{G}(\vec{q}, \tau) = e^{-\frac{T}{2\kappa} \hat{\nu}(q) q^2 \tau} \quad (3.20)$$

where $\hat{\nu}(q) = 1 + (qa_\xi)^{\zeta^{-1}-2}$. This simple form of \hat{G} extrapolates smoothly between the bare function $\hat{G}_0(\vec{q}, \tau) = e^{-\frac{T}{2\kappa} q^2 \tau}$ for $qa_\xi \gg 1$ and the appropriate scaling form (3.9) for $qa_\xi \ll 1$. It is therefore a useful guide to the qualitative features of the crossover. (A better determination of the response function is given in Ref. [26].) Using the bare vertex Eq. (3.14) and the approximate form Eq. (3.20) for \hat{G} , the droplet distribution becomes

$$\hat{W}(\vec{q}, t) = 1 - \frac{1}{\hat{\nu}(q)} \left\{ 1 - e^{-\frac{T}{\kappa} \hat{\nu}(q) q^2 \tau} \right\}, \quad (3.21)$$

with the limiting forms

$$\hat{W}(\vec{q}, \tau) = \begin{cases} 1 - \frac{T}{\kappa} q^2 & \text{for} \quad q < \tau^{-\zeta}, \\ -q^{2-\zeta^{-1}} & \text{for} \quad a_\xi^{-1} > q > \tau^{-\zeta}, \\ e^{-\frac{T}{\kappa} q^2 \tau} & \text{for} \quad q > a_\xi^{-1}. \end{cases} \quad (3.22)$$

Fourier transforming leads to a droplet distribution $W(\vec{\Delta}, \tau)$ sketched in Fig. 7 (solid line), with the asymptotic scaling behavior for $\Delta \gg a_\xi$ given by Eq. (3.16), and a smooth behavior for $\Delta < a_\xi$. It should be emphasized that the precise form of \widehat{G} and $\widehat{\Gamma}_{1,2}$ will change only the details of the crossover function connecting the scaling region to the regions with $\Delta < a_\xi$ and $\Delta > \tau^\zeta$, but not the qualitative features of the distribution. Assuming weak dependence of $W_t(\vec{\Delta}, \tau)$ on t/τ , we expect the distribution $\widetilde{W}(\vec{\Delta}, t)$ for the end point to have the same form (solid line of Fig. 7) with yet another crossover function. Finally, the same considerations lead to a similar form for the distribution of the susceptibility, $D_t(\chi, \tau)$.

B. Glassy Properties of the Pinned Phase

1. Droplet Excitations

We now interpret the results obtained in the previous sections in terms of the structure of ground states and excitations of the randomly-pinned directed polymer. We first compare the result for $W(\vec{\Delta}, \tau)$ in the limit of zero disorder. In this case, the microscopic cutoff length diverges, i.e., $a_\xi \rightarrow \infty$, and the distribution $W^{(0)}(\vec{\Delta}, \tau)$ no longer has a power-law tail and instead takes on a simple gaussian form Eq. (2.19) sketched as the dashed line in Fig. 7. Comparing the solid and the dashed lines, we clearly see that the biggest effect of the disorder is to shift the distribution to the small- Δ end. From Fig. 7, it is clear that most of the samples have $\Delta \ll \tau^\zeta$. In fact, the likely end point separations for typical samples is given by the peak of the distribution which occurs for $\Delta \lesssim a_\xi$. This suggests that *most* samples have a *unique* ground state (and a unique equilibrium state at low T), like the one sketched in Fig. 2(a). Only a small fraction of the samples, of the order

$$U_t(\tau) = \int_{\tau^\zeta}^{2\tau^\zeta} d^d \vec{\Delta} W_t(\vec{\Delta}, \tau) \sim \tau^{-\tilde{\theta}} u(\tau/t), \quad \text{with} \quad \tilde{\theta} = 2\zeta - 1, \quad (3.23)$$

have almost degenerate ground states that are separated by a distance of $O(\tau^\zeta)$ at a distance $\tau \gg a_\tau$ from the fixed end. These are the large scale active droplets excitations depicted in Fig. 2(b). It has been argued in Ref. [18] that $\zeta > 1/2$ for the low temperature phase

of the directed polymer in any finite dimensions. If this is indeed the case, then $\tilde{\theta} > 0$ and from Eq. (3.23) the large droplets are rarely encountered in the thermodynamic limit $\tau \rightarrow \infty$. However, the rare occurrence of these droplets can dominate disorder-averaged thermodynamic quantities due to the diverging sizes of active excitations when they do occur. For instance, it is straightforward to verify that the mean square end point fluctuations, $\overline{C}_T(\tau, t) = \frac{1}{2}\overline{\Delta^2} \sim \tau$, as required by the statistical tilt symmetry Eq. (2.24), is *dominated* by the large droplets in the tail of the distribution $W_t(\vec{\Delta}, \tau)$, i.e., those with $\Delta \sim \tau^\zeta$.

At this point, we should reexamine the identification of $W_t(\vec{\Delta}, \tau)$ with the droplet distribution: In doing so, we made an implicit assumption that configurations with multiple almost-degenerate ground states give negligible contributions in the thermodynamic limit. This is clearly wrong in the absence of disorder. To check the assumption in the presence of disorder, we can compute the probability of having a triply-degenerate ground state, such as the one shown in Fig. 8. Extending the method described in the above sections, we can consider the probability that $P_1(\vec{y}, t_0 | \vec{x}, t)$ has three large peaks at the end point $t_0 = 0$. (The same can be applied to degeneracies in the bulk.) This probability can be obtained from the correlation function $\overline{P_1 P_1 P_1}$. The connected part of this correlation function of the distribution is formally given by $G_{3,1} = \delta^3 \overline{F} / \delta \tilde{J}^3$ and can be computed from the knowledge of G and $\Gamma_{1,2}$ (see the Appendices). The resulting probability of \vec{y}_1, \vec{y}_2 , and \vec{y}_3 all separated by $O(\Delta)$ (Fig. 8), is of order $\Delta^{2d} W^2(\vec{\Delta}, t)$ as one would naively expect from the droplet interpretation. Therefore, the occurrence of triply-degenerate ground states with three end points all $O(t^\zeta)$ away from each other is very rare, of $O(t^{-2\tilde{\theta}})$. One can therefore neglect the effect of such multiply-degenerate ground states for most observables as long as $\tilde{\theta} > 0$, i.e., if $\zeta > 1/2$.

The analysis we have carried out yields information, as we have seen, about the probability of finding large thermally active excitations, i.e., those with excitation free energy δF of order T or smaller. In contrast, the natural quantity that arises in the phenomenological scaling theory [18] is the probability $P_D(\Delta, \delta F)$ of finding an excitation with displacement of

order Δ and free energy $\delta F \sim \Delta^\alpha$ where α is the exponent which controls the magnitude of the free energy variations as the end point $(\vec{y}, 0)$ is moved through distances of order $\Delta \ll t^\zeta$ (Sec.II.D). Since most of the path will change when $\Delta \sim t^\zeta$, then $t^{\zeta\alpha} \sim t^\theta$ is the scale of variations of the free energy (when $\Delta > t^\zeta$), and *also* the variations from sample to sample. The basic scaling hypothesis is that all free energy scales on length scale τ scale as τ^θ and all displacement Δ scale as τ^ζ , so that for $a_\xi \ll \Delta \ll t^\zeta$,

$$P_D(\Delta, \delta F)d(\delta F) \sim \frac{d(\delta F)}{(\delta F)^\alpha} \tilde{p}_D(\delta F/\Delta^\alpha). \quad (3.24)$$

From balancing the change in the *mean* free energy as a function of \vec{y} (which is just $\kappa|\vec{y} - \vec{x}|^2/(2t)$ from the statistical tilt symmetry), with the random part of the free energy as \vec{y} is varied, the exponent identity

$$\theta = 2\zeta - 1 \quad (3.25)$$

is obtained. It was argued in Ref. [18] that the natural form of the scaling function \tilde{p}_D is that it goes to a constant for small argument so that for $T \ll \Delta^\alpha$, the probability of an excitation being thermally active is of order T/Δ^α . Although “natural” and consistent with numerical studies, this does appear as an additional assumption. We now see, however, that the present calculation tells us that it is correct since we have found that

$$P_D(\Delta, \delta F = T) \sim \int_\Delta^{2\Delta} W(\Delta', t)d^d \Delta' \sim \Delta^{-2+\zeta^{-1}}, \quad (3.26)$$

which agrees with the conjectured form. The exponent $\tilde{\theta}$ for active excitations with $\Delta \sim t^\zeta$ is therefore equal to θ . We have thus shown that the exponents describing the probability of the *typical* and the *rare* active excitations are the same! This result is rather important, since its analog has been assumed in a variety of random systems.

Before discussing the physical response functions, we briefly consider what would happen if the wandering exponent ζ were $1/2$. It has been suggested, on the basis of results on the Cayley tree [13], that this might occur for the pinned phase in sufficiently high dimensions. It also occurs at the *critical* point, separating the high and low temperature phases for

$d > 2$ [32]. If $\zeta = 1/2$, but the displacements at a distance τ from the fixed end grow logarithmically faster than $\tau^{1/2}$, then θ would be zero but there will be logarithmic growth of the free energy scale with length scale and, presumably, a $(\log q)^x$ cusp in $\widehat{W}(q, \tau)$ which would yield a distribution of the form $W(\vec{\Delta}, \tau) \sim \Delta^{-d}(\log \Delta)^y$ in the scaling region. In this case, configurations involving multiply degenerate ground states could contribute substantially to disorder averages, and the droplet picture would no longer be simple. If ζ is strictly $1/2$ with no logarithms, the behavior would be even more complicated. Exact calculations on the Cayley tree [13] where this occurs shows that, indeed a finite fraction of samples have nearly degenerate ground states with very little overlap between them. However, many of the properties on the Cayley tree are pathological [18] because two paths never meet again once they branch. At the critical point of the polymer's glass transition for $d > 2$, the free energy scale is of order T because the transition occurs at a finite temperature [32]. Depending on the definition of θ , it may or may not include logarithms [18]. In any case, our considerations based on low free energy excitations must be modified as in Refs. [18] and [33]. The physics of this glass transition is very rich and will be left for future study.

2. Anomalous Linear Response

We now analyze the distribution of the linear response χ . As explained in Sec.III.A, we obtain a power law tail for $D_t(\chi, \tau)$ from assuming that χ is dominated by individual large active droplets of appropriate sizes. What were ignored were contributions to χ from multiply-degenerate ground state configurations such as the one sketched in Fig. 8. But we have shown in Sec.III.B.1 that the probability of the triply degenerate configuration is of order $t^{-\theta}$ lower than that of the doubly degenerate configurations. (Higher order degeneracy should be even rarer.) On the other hand, contributions to χ from a given doubly or triply degenerate configuration are of the same order ($\sim \Delta^2/T$). Thus it is reasonable to neglect the contribution to $D_t(\chi, \tau)$ from higher order degeneracies in the large τ limit. The resulting distribution, which depends solely on the droplet excitations, should then be similar in form

to $W_t(\Delta \sim \sqrt{\chi}, \tau)$ as sketched in Fig. 7 (solid line), with a regular part for small χ and a long tail described by Eq. (3.19) for $\chi \gg (a_\tau/\kappa)^2$. [Again, this would not hold at the critical point or in $d = \infty$ where $\zeta = 1/2$ and $\theta = 0$. In these situations, the multiply-degenerate ground states could contribute to χ at the same order, and the distribution function $D_t(\chi, \tau)$ might be more complicated. It will be interesting to explore these special situations, for example by analyzing the directed polymer on a Cayley tree, or by studying the behavior *at* the glass transition.]

The distribution $D_t(\chi, \tau)$, and in particular, the distribution of the linear response to a uniform field

$$\widetilde{D}(\chi, t) = D_t(\chi, t) \tag{3.27}$$

can be obtained experimentally, by following the domain wall of a planar random Ising magnet in the ordered phase, or by following the end points of flux lines in type-II superconductors close to H_{c1} . This may not seem practical at first glance, as many samples would seem to be required. However, thanks to the special statistical tilt symmetry present in this problem (see also Ref. [33]), the distribution $\widetilde{D}(\chi, t)$ can actually be obtained from a *single* sample. To see this, we just need to realize that the directed polymer only occupies a very limited volume of a given sample. To be more specific, the polymer of length t is essentially contained within a $d + 1$ dimensional ‘‘cone’’ (actually, a distorted paraboloid) of length t and radius t^ζ about the pinned end. So if we apply a uniform tilt field h [Eq. (2.21) with $t_0 = 0$], the polymer will be biased, on average, to tilt by an angle $\phi = h/\kappa$. It is therefore forced out of the cone for

$$h > O(t^{\zeta-1}). \tag{3.28}$$

Once outside of the cone, the polymer encounters a random potential completely different from the one within the cone, since the random potential inside and outside of the cone are uncorrelated. Due to the statistical tilt symmetry, the random part of the new potential the polymer encounters is statistically the same as the one inside the cone. In other words, the

new potential is just like another realization of randomness or another sample except for the trivial mean tilt energy. Therefore, disorder averages can be obtained simply by monitoring the linear response χ as a function of the tilt angle which is varied by changing the applied field h over a range $\delta h \gg t^{\zeta-1}$.

Recently, Mézard [20] reported such a numerical study of the polymer's response as a function of the applied tilt field h , for a fixed realization of the random potential in 1+1 dimensions. Qualitatively, the position of the free end $y(h) = \langle \xi(0) \rangle_h$ is found to be *independent* of h for a range of the applied field. But $y(h)$ can “jump”, by a distance of $O(t^{2/3})$ for a polymer of length t , if the applied field is increased by $O(t^{-1/3})$. As a result, the response $\chi(h) = dy(h)/dh$ exhibits a series of sporadic sharp peaks, with strengths of $O(t^{4/3})$, separated by distances of $O(t^{-1/3})$, yielding $\bar{\chi} \sim t$ on average. (Here the average is performed over the applied field, i.e., by $\frac{1}{h} \int_0^h dh' \chi(h')$ for $h \gg t^{-1/3}$.)

The above qualitative findings are of course consistent with the droplet picture described in this paper. As expected, a directed polymer in a typical realization of the random potential (or at some given tilt field) has an unique ground state. Typical excited states with distances $O(t^\zeta)$ away are of $O(t^\theta)$ higher in free energy. This “energy gap” prohibits any large scale response to a very small increase in the field h . Since the applied field supplies an energy $\vec{h} \cdot (\vec{\xi}(t) - \vec{\xi}(0)) \sim ht^\zeta$, the “energy gap” can be overcome for $ht^\zeta > t^\theta$. This is just the condition Eq. (3.28) using the exponent relation Eq. (3.25). In 1+1 dimensions, we have $\zeta = 2/3$. Thus the energy gap is overcome and the end point jumps when $h \sim t^{-1/3}$. By the statistical tilt symmetry, the process repeats itself (statistically) once the polymer's end point “jumps” by $O(t^\zeta)$. This then produces the sporadic jumps in $y(h)$ [or peaks in $\chi(h)$] observed in Ref. [20].

One might wonder why there are not many jumps of size $\Delta \ll t^\zeta$, involving just a section of length $\Delta^{1/\zeta}$ near the free end. These typically cost energy of order Δ^α and gain field energy of order $\delta h \Delta$. Thus naively, they will occur when $\delta h \sim 1/\Delta^{1-\alpha}$. However, since this increases with decreasing Δ , small jumps will almost always be preempted by large jumps. They will only occur if the excitation energy is anomalously small [of order $\Delta/t^{1-\zeta}$

which occurs with probability $(\Delta/t^\zeta)^{1-\alpha}$. Therefore most of the end point motion as a function of h will occur in jumps of $O(t^\zeta)$.

It should be possible to get some analytical information on the distribution of *jumps* from the methods of the paper, but the details are complicated. One would need information on joint distribution of end points with slightly different tilt fields \vec{h}_1 and \vec{h}_2 , but the same random potential, such as

$$\overline{P_1(\vec{y}_1, 0|\vec{x}, t; \vec{h}_1)P_1(\vec{y}_2, 0|\vec{x}, t; \vec{h}_2)}. \quad (3.29)$$

Conceptually, studying the response χ of a system by slowly varying an uniform bias \vec{h} is similar to recent studies of self-organized criticality in cellular automaton models of sandpiles [34,35] and earthquakes [36]: Tilting the polymer corresponds to tilting the sandpile or increasing the loading force on a fault in earthquake models. Anomalously large responses (the sporadic peaks in $\chi(h)$) exhibited by the polymers are like the “avalanches” encountered in the cellular automaton models. Of course, there are fundamental differences: The present study addresses *equilibrium* fluctuations of a disordered system at low temperatures, while the cellular automaton models mimic the *nonequilibrium* dynamics at zero temperature. In particular, if a directed polymer in a random potential with relaxational dynamics at zero temperature is driven by increasing the tilt bias adiabatically, the spectrum of avalanches, i.e., jumps, will be very different from the equilibrium behavior discussed above: There will be many small avalanches and only occasionally large ones, as analyzed for higher dimensional driven manifolds by Narayan and Fisher [37]. In addition, as h is increased, the polymer will stay in configurations that for a while become more and more strained with the free end advancing much faster than the midpoint, in contrast to the equilibrium case. Nevertheless, the two problems share the key feature of a broad distribution of large rare “events”. Intuition gained from studying the equilibrium behavior may therefore provide useful hints for understanding the nonequilibrium problem.

IV. DISCUSSION

In this paper, we have presented a systematic investigation of some properties of the large scale, low energy excitations of directed polymers in random media. The large scale thermally active excitations occur in a small fraction of samples (or regions of a sample) which have almost degenerate ground states that differ by large displacement in the region. We showed the probability of occurrence of such samples, with excitations on scale t , is of order $t^{-\theta}$ in the limit the polymer length $t \rightarrow \infty$. Nevertheless, many of the disorder-averaged thermodynamic properties are dominated entirely by these rare samples. This is because in most of the samples, a polymer is essentially frozen in a unique ground state, with the largest scale excitations having energy of order t^θ hence not being thermally active. The rare samples with large active excitations make up for their small numbers by displaying anomalously large fluctuations which dominate the mean. We computed the distribution of the almost degenerate ground states for a polymer with one end fixed. While the distribution is peaked at small separations, we found a long power-law tail describing almost degenerate configurations that are far apart, with separation Δ at a distance τ from the fixed end ranging from zero to the maximum important extent τ^ζ (with rapid decay for $\Delta \gg \tau^\zeta$). This distribution of almost degenerate configurations also provides information on the distribution of excitations on scales much *less* than the system size which dominate many of the properties of large systems.

The analysis was carried out by exploiting the known mapping of the directed polymer to the noisy Burgers equation, which converted singular, rare fluctuations to smooth, hydrodynamic fluctuations. We found that the interesting polymer distribution functions corresponded to various response functions of the Burgers' equation, and the tails of the distributions, which are generally difficult to obtain, are in this case just the hydrodynamic limits of the response functions and therefore much more straightforward to analyze. In the context of the Burgers' equation, the power law tails are merely the "long time tails" that are well known in hydrodynamic systems. Most of the difficulties with analyzing the properties

of the pinned phase of the directed polymer by conventional methods are due to its control by a non-trivial randomness-dominated zero-temperature fixed point at which temperature is “dangerously irrelevant”, meaning that interesting correlation functions *cannot* be obtained by setting T to zero. The main advantage of the approach via the noisy-Burgers’ equation, is that the problem is converted into a much more conventional one in which fluctuations play the dominant role and field theoretic methods can be used. The physics of minimization of the coarse grained free energy to find “ground states” and then treatment of the anomalous rare fluctuations around the ground states miraculously appear as a consequence of the existence of a conventional fixed point of the hydrodynamic problem.

Our findings support the main conjectures of the droplet theory [18,19]. What we have demonstrated in this paper is a formal way of obtaining the statistics of the active droplets and various direct physical consequences of their distributions. As should be clear from the derivation of the distribution functions, a crucial ingredient which leads to power-law tails of distributions is the existence of the statistical tilt symmetry. It is thus tempting to attribute the scale-invariant distributions to some analog of the Goldstone modes associated with the tilt symmetry for the *ensemble* of disordered systems which is “spontaneously-broken” by the selection of the configuration for each specific sample. It would be important to understand whether in general such a symmetry is sufficient to ensure the existence of a power-law tail of large rare fluctuations in disordered systems controlled by randomness-dominated zero-temperature fixed points.

The large rare thermally active excitations in the pinned phase of random directed polymers are closely analogous to the droplet excitations proposed to describe the low temperature phase of Ising spin glasses. Their existence in spin glasses was argued to depend, as in the present case, on the existence of a non-trivial zero temperature fixed point which is *stable* to thermal fluctuations [10]. This stability to fluctuations — and thus the whole picture — occur only when the free energy exponent θ is positive (or perhaps zero with logarithms). But what is the analog of the statistical tilt symmetry for spin glasses ? In the Edwards-Anderson model, there is a statistical local gauge symmetry associated with

changing the sign of one spin and all the exchange couplings involving that spin. This was used, implicitly, to argue for the existence of large rare thermally active excitations in spin glasses [10]. It plays a role analogous to the statistical tilt symmetry of the directed polymer. Note however that the statistical gauge symmetry is not exact in more realistic models of spin glasses in which ferro and antiferromagnetic exchanges are not equally likely. Nevertheless, it is believed that in the spin glass phase, the deviations from the exact symmetry are irrelevant on long length scales. A similar phenomenon occurs for directed polymers on a *lattice* in which there are short-distance correlations in the random potential along the polymer. In this case, the statistical tilt symmetry is *not* exact but numerical evidence support the conjecture that the deviations from it are irrelevant at long length scales.

It is finally useful to compare this study with a recent uncontrolled field-theoretic analysis using replicas. In principle, distribution functions such as $W_t(\vec{\Delta}, \tau)$ can be obtained using the replica method [17]. However, difficulties arise in trying to take the $n \rightarrow 0$ limit which is not uniquely defined from the positive integer n . Mézard and Parisi have proposed a gaussian variational ansatz [17] to treat the directed polymer problem. Within this framework, it is easy to see that replica-symmetry must be broken in order to recover the rare fluctuations. In such a treatment, the branching tree structure of ground states as a function of their end points in physical space (Fig. 6) is replaced by an abstract hierarchical “family” tree structure in replica space. The key to the power-law tails of the distribution functions is the overlap of “distant family members”, the $u \rightarrow 0$ limit of the function $[\sigma](u)$ in the notation of Ref. [17]. Within the gaussian ansatz, a nontrivial tail is obtained if $[\sigma](u \rightarrow 0) \rightarrow u^{2/\theta}$. Thus the replica-symmetry breaking scheme seems to be an approximate way of obtaining rare fluctuations within the replica formalism [39]. As such, it *may* be a useful tool for other problems. However, the variational approximation is uncontrolled and the physics enters in a very roundabout manner. It is thus not at all clear why this approach has any advantages over a direct phenomenological scaling approach as in Ref. [18], renormalization group calculations which are exact on the hierarchical lattice [14], or approximate “functional” renormalization group studies [7,38], all of which have the real

virtue that the physics appears directly. Furthermore, it is not clear if *any* real physics is associated with the notion of “replica-symmetry breaking” [39]. As our study implies, the power-law tail of the rare fluctuations are a rather general consequence of the statistical symmetry of the problem; the ill-defined concept of “replica-symmetry breaking” is of course not needed at all in our analysis [40] ! However, the simple structure of the free energy functional via the noisy-Burgers’ equation, relies *strongly* on the one-dimensional nature of the directed polymer. It will be very interesting to see if our method can be extended, using the formalism of Appendix A, to study higher (but finite) dimensional systems such as oriented manifolds in random media [7].

It may be comforting to some to find that the important physics of the ground state, — in particular power-law distributions of rare, anomalously large fluctuations — can be retrieved both by analysis in physical and replica space. For the directed polymer, at least, there are no substantial disagreement between these two approaches. It is possible that controversies regarding the nature of the low-temperature phase of finite-dimensional spin-glasses may have a similar resolution, with the many thermodynamic “states” of the infinite-range Sherrington-Kirkpatrick model becoming, in finite dimensions, just the large scale, low free energy droplet excitations of the phenomenological scaling approach.

ACKNOWLEDGMENTS

We are grateful to many helpful discussions with E. Frey, V. L'vov, and T. Nattermann, and also thank P. W. Anderson and G. Parisi for insightful comments. TH acknowledges the hospitality of NORDITA where part of this work was completed. This work was supported in part by the National Science Foundation through Grants Nos. DMR-91-06237, DMR-91-15491 and the Harvard University Materials Research Laboratory.

APPENDIX A: A FIELD THEORY FOR RANDOM SYSTEMS

In this Appendix, we consider a general field theoretic description of manifolds in random media. In particular, we study a disordered system described by a Hamiltonian $\mathcal{H}[\vec{\xi}(\underline{z}), \eta]$ which is defined on the D -dimensional manifold $\underline{z} \in \mathfrak{R}^D$, with $\vec{\xi} \in \mathfrak{R}^d$ a d -component ‘‘order parameter’’, and $\eta(\vec{\xi}, \underline{z})$ a quenched random variable (in our case the potential) distributed according to some distribution $p[\eta]$. The one-point restricted partition function is

$$Z(\vec{x}, \underline{t}; \eta) = \int \mathcal{D}[\vec{\xi}] \delta^d(\vec{\xi}(\underline{t}) - \vec{x}) e^{-\mathcal{H}[\vec{\xi}, \eta]/T}. \quad (\text{A1})$$

Various distribution functions can be obtained by adding a source term

$$\mathcal{H} \rightarrow \mathcal{H} + \int d^D \underline{z} \tilde{J}(\vec{\xi}, \underline{z}), \quad (\text{A2})$$

and then differentiating the free energy,

$$F(\vec{x}, \underline{t}; \tilde{J}; \eta) = -T \log Z(\vec{x}, \underline{t}; \tilde{J}; \eta). \quad (\text{A3})$$

For instance,

$$\frac{\delta \bar{F}(\vec{x}, \underline{t}; \tilde{J})}{\delta \tilde{J}(\vec{x}_1, \underline{t}_1)} = \overline{\langle \delta^d(\vec{\xi}(\underline{t}_1) - \vec{x}_1) \rangle}, \quad (\text{A4})$$

which is the disorder-averaged conditional probability of $\vec{\xi}(\underline{t}_1) = \vec{x}_1$ given $\vec{\xi}(\underline{t}) = \vec{x}$, and

$$\frac{\delta^2 \bar{F}(\vec{x}, \underline{t}; \tilde{J})}{\delta \tilde{J}(\vec{x}_1, \underline{t}_1) \delta \tilde{J}(\vec{x}_2, \underline{t}_2)} = -\frac{1}{T} \overline{\langle \delta^d(\vec{\xi}(\underline{t}_1) - \vec{x}_1) \delta^d(\vec{\xi}(\underline{t}_2) - \vec{x}_2) \rangle}^{(c)}, \quad (\text{A5})$$

where the notations for thermal and disorder averages are the same as those used in Sec.II.A, and the superscript (c) denotes the connected (or truncated) correlations. We will generally be interested in the n^{th} order distribution and correlation functions,

$$\mathcal{G}_{n,1}^{(c)}(\mathbf{x}_1; \dots; \mathbf{x}_n | \mathbf{x}) = \frac{\delta^n \bar{F}(\mathbf{x}; \tilde{J})}{\delta \tilde{J}(\mathbf{x}_1) \dots \delta \tilde{J}(\mathbf{x}_n)}, \quad (\text{A6})$$

and

$$\mathcal{G}_{0,n}^{(c)}(\mathbf{x}_1; \dots; \mathbf{x}_n) = \overline{F(\mathbf{x}_1) \dots F(\mathbf{x}_n)}, \quad (\text{A7})$$

where we have used the shorthand $\mathbf{x}_i = (\vec{x}_i, \underline{t}_i)$. Clearly, translational symmetry in space (\vec{x} 's) is restored upon disorder average. In addition, if we consider a very large manifold where the boundary of \underline{z} is far from any of the distances $\underline{t}_i - \underline{t}_0$, then we also have translational symmetry in the internal coordinates. For a semi-infinite polymer, this leads to $\mathcal{G}_{1,1}^{(c)}(\vec{y}, t - t_1 | \vec{x}, t) = G(\vec{x} - \vec{y}, t - t_1)$, which is just the one-point distribution function $\overline{P}_1(\vec{y}, t_1 | \vec{x}, t)$. Also, $\mathcal{G}_{0,2}^{(c)}(\vec{x}, t; \vec{y}, t)$ is related to the free-energy correlation function $C_F(\vec{x} - \vec{y}, t)$ in Eq. (2.28), and $\mathcal{G}_{2,1}^{(c)}(\vec{y}_1, t_1; \vec{y}_2, t_1 | \vec{x}, t) = G_{2,1}(\vec{x} - \vec{y}_1, \vec{x} - \vec{y}_2, t - t_1)$ gives the droplet distribution through Eq. (3.5).

To carry out the average over disorder, it is advantageous to eliminate the random variables $\eta(\mathbf{x})$ in favor of a probability density for the field $F(\mathbf{x})$ itself, i.e.,

$$\widehat{\Xi}[F, \tilde{J}] = \int \mathcal{D}[\eta] \delta(F + T \log Z[\tilde{J}; \eta]) p[\eta], \quad (\text{A8})$$

so that the mean free energy is

$$\overline{F}(\mathbf{x}; \tilde{J}) = \int \mathcal{D}[F] F(\mathbf{x}) \widehat{\Xi}[F, \tilde{J}]. \quad (\text{A9})$$

It will be more convenient to write $\widehat{\Xi}$ in terms of its (functional) Fourier transform $\Xi[\tilde{F}, F]$ as

$$\widehat{\Xi}[F, \tilde{J}] = \int \mathcal{D}[i\tilde{F}] \Xi[\tilde{F}, F] e^{\int d\mathbf{x} \tilde{J}(\mathbf{x}) \tilde{F}(\mathbf{x})}. \quad (\text{A10})$$

Note that Eq. (A10) is similar to the dynamic generating functional of Martin, Siggia and Rose [31,41] with \tilde{F} being the “response field”. For a generic random system, the free energy functional $\Xi[\tilde{F}, F]$ will in general be rather complicated. However, the one-dimensional nature of the directed polymer can be exploited [2,3] to derive a functional that is *local* in F and \tilde{F} . The explicit form of $\Xi[\tilde{F}, F]$ is shown in Appendix B.

After adding a source term to Eq. (A10) to generate correlations of F , we obtain the generating functional

$$\mathcal{Z}[J, \tilde{J}] = \int \mathcal{D}[i\tilde{F}] \mathcal{D}[F] \Xi[\tilde{F}, F] \exp \left[\int d\mathbf{x} \left(\tilde{J}(\mathbf{x}) \tilde{F}(\mathbf{x}) + J(\mathbf{x}) F(\mathbf{x}) \right) \right]. \quad (\text{A11})$$

The distribution and correlation functions of interest can now be obtained from functional derivatives of $\Phi[\tilde{J}, J] \equiv \log \mathcal{Z}[\tilde{J}, J]$, e.g.,

$$\begin{aligned} \mathcal{G}_{m,n}^{(c)}(\mathbf{y}_1; \dots; \mathbf{y}_m | \mathbf{x}_1; \dots; \mathbf{x}_n) &= \frac{\delta^{m+n} \Phi[\tilde{J}, J]}{\delta \tilde{J}(\mathbf{y}_1) \dots \delta \tilde{J}(\mathbf{y}_m) \delta J(\mathbf{x}_1) \dots \delta J(\mathbf{x}_n)} \\ &= \overline{\tilde{F}(\mathbf{y}_1) \dots \tilde{F}(\mathbf{y}_m) F(\mathbf{x}_1) \dots F(\mathbf{x}_n)}^{(c)}, \end{aligned}$$

where the disorder average (overbar) is now performed using $\mathcal{Z}[J = 0, \tilde{J} = 0]$.

Note that the normalization of $\hat{\Xi}[F, \tilde{J}]$ requires $\mathcal{Z}[J = 0, \tilde{J}] = 1$. Hence all of the moments $\mathcal{G}_{m,0}^{(c)} = 0$. To obtain the other moments, we introduce the vertex functions [42],

$$\gamma_{m,n}(\mathbf{y}_1; \dots; \mathbf{y}_m | \mathbf{x}_1; \dots; \mathbf{x}_n) = \frac{\delta^{m+n} \Gamma[\tilde{F}, \overline{F}]}{\delta \tilde{F}(\mathbf{y}_1) \dots \delta \tilde{F}(\mathbf{y}_m) \delta \overline{F}(\mathbf{x}_1) \dots \delta \overline{F}(\mathbf{x}_n)}, \quad (\text{A12})$$

where $\Gamma[\tilde{F}, \overline{F}]$ is the Legendre transform of Φ :

$$\Gamma[\tilde{F}, \overline{F}] = \int d\mathbf{x} \left[\tilde{F}(\mathbf{x}) \tilde{J}(\mathbf{x}) + \overline{F}(\mathbf{x}) J(\mathbf{x}) \right] - \Phi[\tilde{J}, J], \quad (\text{A13})$$

with \tilde{J} and J eliminated from the above expression using

$$\tilde{F} = \frac{\delta \Phi}{\delta \tilde{J}}, \quad \overline{F} = \frac{\delta \Phi}{\delta J}. \quad (\text{A14})$$

It is a simple exercise to show that all of the correlation functions $\mathcal{G}_{m,n}^{(c)}$ can be obtained from the vertex functions $\gamma_{m,n}$ [42]. The advantage of introducing the vertex functions is to allow the derivation of Ward identities from symmetries [42]. This will be done in Appendix C.

With $\mathcal{G}_{m,0}^{(c)} = 0$, the expressions for $\mathcal{G}_{m,1}^{(c)}$ are particularly simple: Only the connected parts survive (we will therefore drop the superscript (c)), and all of the higher order functions $\mathcal{G}_{m,1}$ can be obtained from the combination of $\gamma_{1,m}$'s and $\mathcal{G}_{1,1}$. For instance,

$$\int d\mathbf{x} \mathcal{G}_{1,1}(\mathbf{y} | \mathbf{x}) \gamma_{1,1}(\mathbf{x} | \mathbf{y}') = \delta(\mathbf{y} - \mathbf{y}'), \quad (\text{A15})$$

thus $\gamma_{1,1}$ is the inverse ‘‘propagator’’, and

$$\mathcal{G}_{2,1}(\mathbf{y}_1; \mathbf{y}_2 | \mathbf{x}) = - \int d\mathbf{x}' d\mathbf{y}'_1 d\mathbf{y}'_2 \mathcal{G}_{1,1}(\mathbf{x}' | \mathbf{x}) \gamma_{1,2}(\mathbf{x}' | \mathbf{y}'_1; \mathbf{y}'_2) \mathcal{G}_{1,1}(\mathbf{y}_1 | \mathbf{y}'_1) \mathcal{G}_{1,1}(\mathbf{y}_2 | \mathbf{y}'_2). \quad (\text{A16})$$

This leads to Eq. (3.6) for the directed polymer with $\mathcal{G}_{1,1}(\mathbf{x}'|\mathbf{x}) = G(\mathbf{x}-\mathbf{x}')$, $\mathcal{G}_{2,1}(\mathbf{y}_1;\mathbf{y}_2|\mathbf{x}) = G_{2,1}(\vec{x} - \vec{y}_1, \vec{x} - \vec{y}_2, \tau)$, and $\gamma_{1,2}(\mathbf{x}'|\mathbf{y}'_1;\mathbf{y}'_2) = \Gamma_{1,2}(\vec{x}' - \vec{y}'_1, t' - t'_1; \vec{x}' - \vec{y}'_2, t' - t'_2)$ due to the translational symmetry in a semi-infinite polymer after averaging over the disorder. The result Eq. (A16) is conveniently represented by a tree diagram (Fig. 6). A higher order distribution function $\mathcal{G}_{m,1}$ typically contains a tree diagram involving only $\gamma_{1,2}$ and $\mathcal{G}_{1,1}$, plus diagrams involving higher order vertex functions $\gamma_{1,m'}$, with $2 < m' \leq m$. An even larger class of vertex functions are needed to generate the correlation functions, $\mathcal{G}_{0,n}$'s. The description of these is more complicated, and we will not discuss them except to note that for the directed polymer in $1 + 1$ dimensions, there exists identities (fluctuation-dissipation theorems) linking $\mathcal{G}_{0,n}$ and $\mathcal{G}_{n,1}$ [26,43].

APPENDIX B: MAPPING TO STOCHASTIC DYNAMICS

In this appendix, we describe a mapping of the random directed polymer to a stochastic dynamics problem — the noisy Burgers’ equation — first noted in Ref. [2]. We show how this mapping can be used to extract information about the directed polymer, and thereby provide a concrete example of the general field theoretic method described in Appendix A.

Let us consider the doubly-restricted partition function

$$Z_2(\vec{x}, t; \vec{x}', 0) = \int \mathcal{D}[\vec{\xi}] \delta^d(\vec{\xi}(t) - \vec{x}) \delta^d(\vec{\xi}(0) - \vec{x}') e^{-\mathcal{H}/T} \quad (\text{B1})$$

where (\vec{x}, t) and $(\vec{x}', 0)$ are the end point locations of a directed polymer of length t . We see that Z_2 is the Boltzmann weight of “propagating” the polymer from $(\vec{x}', 0)$ to (\vec{x}, t) ; it satisfies the “diffusion” equation

$$T \frac{\partial}{\partial t} Z_2(\vec{x}, t; \vec{x}', 0) = \frac{T^2}{2\kappa} \vec{\nabla}_{\vec{x}}^2 Z_2 - \eta(\vec{x}, t) Z_2, \quad (\text{B2})$$

where t is interpreted as “time” and $(\vec{x}', 0)$ is merely a parameter, which enters through the initial condition $Z_2(x, t = 0; x', 0) = \delta^d(\vec{x} - \vec{x}')$. Since Eq. (B2) is linear, we can easily integrate over the coordinate \vec{x}' to obtain the same diffusion equation for $Z(\vec{x}, t) \equiv \int d^d \vec{x}' Z_2(\vec{x}, t; \vec{x}', 0)$, but now with the initial condition $Z(\vec{x}, 0) = 1$. Then the free energy of the one-point restricted polymer, $F(\vec{x}, t) = -T \log Z(\vec{x}, t)$ satisfies the well-known noise-driven Burgers’ equation [11,12],

$$\frac{\partial F}{\partial t} = \frac{T}{2\kappa} \vec{\nabla}^2 F - \frac{1}{2\kappa} (\vec{\nabla} F)^2 + \eta(\vec{x}, t), \quad (\text{B3})$$

with the initial condition $F(\vec{x}, 0) = 0$. Note that the path integral description of the directed polymer, i.e., Eqs. (2.1) and (2.3), is very different in form, from the dynamic description Eq. (B3) [12]. The task of global optimization presented in the original directed polymer problem is turned into a step-by-step recursive process: Eq. (B3) relates the free energy of a polymer of length t to one of length $t + dt$ and is thus a transfer matrix description of the problem [40].

The noisy-Burgers equation Eq. (B3) itself has been the focus of several recent studies [43]. However, despite much effort, no systematic solution has been found. The lone exception is in 1+1 dimensions, where Eq. (B3) can be thought of as the $d = 1$ limit of an anisotropic driven diffusion equation [44,45]

$$\begin{aligned} \partial_t \phi &= \frac{T}{2\kappa} \nabla^2 \phi - \frac{1}{2\kappa} \partial_x (\phi)^2 + \eta'(\vec{r}, t), \\ \text{with } \langle \eta'(\vec{r}, t) \eta'(\vec{r}', t') \rangle &= -2D \nabla^2 \delta^d(\vec{r} - \vec{r}') \delta(t - t'), \end{aligned} \quad (\text{B4})$$

where x is one particular component of \vec{r} . Eq. (B4) is equivalent to Eq. (B3) in $d = 1$ with the identification $\phi = \partial F / \partial x$ and $\eta' = \partial \eta / \partial x$. [See Ref. [46] for a detailed discussion of the connections between Eq. (B3) and Eq. (B4).] Eq. (B4) has also been investigated in detail [44,45]. It can be solved perturbatively via a $d = 2 - \epsilon$ renormalization group expansion. Furthermore, all of the scaling exponents can be obtained exactly in all d , owing to the existence of a “fluctuation-dissipation theorem” which we shall not elaborate here. One obtains the directed polymer results $\zeta = 2/3$ and $\theta = 1/3$ which we have referred to several times in the text. Not much is known analytically of the noisy-Burgers’ equation away from 1+1 dimensions. Recently, an uncontrolled mode-coupling approach [47,48] along the line of Ref. [26] has been applied to solve Eq. (B3) in 2+1 dimensions, yielding exponent values that are rather close to those obtained from numerical simulations [43]. However, a controlled solution is yet to be developed.

Although quantitative solution (e.g., the exponent values) of the noisy-Burgers’ equation are not available for $d \neq 1$, we can still learn much about the qualitative behavior of the directed polymer, e.g., the rare fluctuations, by exploiting this mapping to hydrodynamics, and especially by exploiting symmetries, as we now describe. From the standard dynamic field theory formulation of Langevin dynamics upon averaging over η [31,41], one can turn Eq. (B3) into the free-energy functional used in Eq. (A11),

$$\Xi[\tilde{F}, F] = e^{-S[\tilde{F}, F]}, \quad (\text{B5})$$

where

$$S[\tilde{F}, F] = \int dt d^d \vec{x} \left[-D \tilde{F}^2(\vec{x}, t) + \tilde{F}(\vec{x}, t) \left(\partial_t F(\vec{x}, t) - \frac{T}{2\kappa} \vec{\nabla}^2 F + \frac{1}{2\kappa} (\vec{\nabla} F)^2 \right) \right]. \quad (\text{B6})$$

Since the disorder potential η has already been averaged out, translational symmetries in both \vec{x} and t are restored in the limit of large t , corresponding to the hydrodynamic steady state. It is then convenient to go to Fourier space, where

$$S[\tilde{F}, F] = \int \frac{d\omega}{2\pi} \frac{d^d \vec{k}}{(2\pi)^d} \left[-D |\tilde{F}(\vec{k}, \omega)|^2 + \left(\frac{T}{2\kappa} k^2 - i\omega \right) \tilde{F}(-\vec{k}, -\omega) F(\vec{k}, \omega) \right] \quad (\text{B7})$$

$$+ \int \frac{d\omega_1}{2\pi} \frac{d\omega_2}{2\pi} \frac{d^d \vec{k}_1}{(2\pi)^d} \frac{d^d \vec{k}_2}{(2\pi)^d} \left(-\frac{1}{2\kappa} \vec{k}_1 \cdot \vec{k}_2 \right) \tilde{F}(-\vec{k}_1 - \vec{k}_2, -\omega_1 - \omega_2) F(\vec{k}_1, \omega_1) F(\vec{k}_2, \omega_2).$$

The functional $S[\tilde{F}, F]$ is called the dynamic functional in the study of stochastic dynamics [41]. In the absence of randomness, i.e., for $D = 0$, this is just the “bare” generating functional of the vertex functions,

$$S[\tilde{F}, F] = \Gamma^{(0)}[\tilde{F}, F]. \quad (\text{B8})$$

From the definition of the vertex functions (A12), we have

$$\Gamma[\tilde{F}, F] = \sum_{m,n} \frac{1}{m!n!} \int_{(\vec{k}, \omega)} \hat{\Gamma}_{m,n} \tilde{F}^m F^n, \quad (\text{B9})$$

where $\hat{\Gamma}_{m,n}$ is the Fourier transform in \vec{x} , \vec{y} and t of the function $\gamma_{m,n}$ in Eq. (A12). Comparing the above to Eq. (B7), we can easily read off the bare vertex functions,

$$\hat{\Gamma}_{1,1}^{(0)}(\vec{k}, \omega) = \frac{T}{2\kappa} k^2 - i\omega, \quad (\text{B10})$$

$$\hat{\Gamma}_{1,2}^{(0)}(\vec{k}_1, \omega_1; \vec{k}_2, \omega_2) = -\frac{1}{\kappa} \vec{k}_1 \cdot \vec{k}_2, \quad (\text{B11})$$

$$\hat{\Gamma}_{2,0}^{(0)}(\vec{k}, \omega) = 0. \quad (\text{B12})$$

The relevance of the random potential in the pinned phase makes the renormalized functional $\Gamma[\tilde{F}, \overline{F}]$ much more complicated. However, we will show in Appendix C that, as a consequence of the statistical tilt symmetry, the *scaling* behavior obtained from $\Gamma_{1,2}^{(0)}$ and $\Gamma_{1,2}$ are the same. This permits us to use the bare vertex $\Gamma_{1,2}^{(0)}$ in place of the full vertex $\Gamma_{1,2}$ to compute the tail of the droplet distribution $W(\vec{\Delta}, \tau)$ in Sec.III.A.

As shown in Sec.III.A, $W(\vec{\Delta}, \tau)$ is obtained by adding a source term \tilde{J} to the random potential η , and then following the changes in \overline{F} . In the context of stochastic dynamics, this procedure amounts to probing the “response” of the hydrodynamic field \overline{F} to a small “perturbation” \tilde{J} added to the right-hand side of Eq. (B3). We see that the distribution functions $\delta\overline{F}/\delta\tilde{J} = G$ and $\delta^2\overline{F}/\delta\tilde{J}^2 = G_{2,1}$ are simply the linear and nonlinear response functions of the noisy-Burgers’ equation. Furthermore, the *tails* of the distribution functions are similarly related to the hydrodynamic limits of the response functions. Thus the mapping to hydrodynamics provides us with a convenient way of approaching the tails of distributions.

APPENDIX C: STATISTICAL TILT SYMMETRY AND WARD IDENTITIES

In this Appendix, we review the statistical tilt symmetry which was used in Ref. [29] to prove the result $\bar{\chi} = \tau/\kappa$. The analogous symmetry in the noisy-Burgers' equation is the Galilean invariance. It has been used in Refs. [11,12] to derive the exponent identity $\theta = 2\zeta - 1$. Here we shall derive the consequences of this symmetry, i.e., Ward identities, more formally. The result is used to compute the droplet distribution in Sec.III.A.

We start with the Hamiltonian $\mathcal{H}[\vec{\xi}, \eta]$ given in Eq. (2.1). Consider the effect of an arbitrary bias of the form

$$\mathcal{H}_h[\vec{\xi}, \eta] = \mathcal{H}[\vec{\xi}, \eta] - \int_0^t dz \vec{h}(z) \cdot \frac{d\vec{\xi}}{dz}. \quad (\text{C1})$$

By a simple coordinate transformation $\vec{\xi}'(z) = \vec{\xi}(z) - \vec{r}(z)/\kappa$, where $\vec{r}(z) = \int^z dz' \vec{h}(z')$, we obtain

$$\mathcal{H}_h[\vec{\xi}, \eta] = \mathcal{H}[\vec{\xi}', \tilde{\eta}] - \frac{1}{2\kappa} \int_0^t dz' \vec{h}^2(z'), \quad (\text{C2})$$

with a transformed random potential

$$\tilde{\eta}(\vec{\xi}', z) \equiv \eta[\vec{\xi}'(z) + \vec{r}(z)/\kappa, z]. \quad (\text{C3})$$

Similarly the free energy of the polymer with a point fixed at $\vec{\xi}(t) = \vec{x}$ is given by

$$F_h(\vec{x}, t; \eta) = F(\vec{x} - \vec{r}(t)/\kappa, t; \tilde{\eta}) - \frac{1}{2\kappa} \int_0^t dz \vec{h}^2(z). \quad (\text{C4})$$

Note that since the random potential η is gaussian and uncorrelated, the distribution of $\tilde{\eta}$ is also gaussian, characterized by its covariance

$$\begin{aligned} \overline{\tilde{\eta}(\vec{x}_1, t_1) \tilde{\eta}(\vec{x}_2, t_2)} &= \overline{\eta(\vec{x}_1, t_1) \eta(\vec{x}_2, t_2)} \\ &= 2D \delta^d(\vec{x}_1 - \vec{x}_2) \delta(t_1 - t_2). \end{aligned} \quad (\text{C5})$$

Thus disorder averages of a functional of F over η and $\tilde{\eta}$ are identical. In particular, if we choose $\vec{h}(z) = \vec{h}$ for $t_0 < z < t$, and $\vec{h}(z) = 0$ for $0 < z < t_0$, then Eq. (C1) reduces to Eq. (2.21), and Eqs. (C4) and (C5) imply that the disorder-averaged linear response is just

$$\bar{\chi} = -\frac{\partial}{\partial h_i^2} \bar{F}_h(\vec{x}, t) \Big|_{\vec{h}=0} = \frac{t - t_0}{\kappa}. \quad (\text{C6})$$

This result was first proved for a class of disordered systems in Ref. [29].

In the following, we shall exploit this statistical symmetry more formally by considering in detail the case $t_0 = 0$, corresponding to applying a uniform tilt field \vec{h} . In this case, Eqs. (C3) and (C4) become

$$\tilde{\eta}(\vec{\xi}, z) \equiv \eta[\vec{\xi}(z) + \vec{h}z/\kappa, z], \quad (\text{C7})$$

and

$$F_h(\vec{x}, t; \eta) = F(\vec{x} - \vec{h}t/\kappa, t; \tilde{\eta}) - \frac{\vec{h}^2}{2\kappa}t. \quad (\text{C8})$$

From Eq. (C8), it is clear that F_h no longer satisfies the noisy-Burgers' equation (B3). However, the combination $F_h(\vec{x}, t) - T\vec{h} \cdot \vec{x}$ does. This is because Eq. (B3) is invariant under the ‘‘Galilean’’ transformation

$$F'(\vec{x}, t) = F(\vec{x} + \vec{v}t, t) - \kappa\vec{v} \cdot \vec{x}, \quad (\text{C9})$$

and

$$\eta'(\vec{x}, t) = \eta(\vec{x} + \vec{v}t, t), \quad (\text{C10})$$

as can be verified straightforwardly for $\vec{v} = \vec{h}/\kappa$. We now use this Galilean invariance to derive some useful Ward identities.

The statistical tilt symmetry implies that the generating functional of the vertex function $\Gamma[\overline{\overline{F}}, \overline{F}]$ is invariant under the Galilean transformation of the disorder-averaged fields \overline{F} and $\overline{\overline{F}}$. In Fourier space, the transformation reads,

$$\overline{F}'(\vec{q}, t_1) = e^{i\vec{v} \cdot \vec{q}t_1} \overline{F}(\vec{q}, t) + i\kappa\vec{v} \cdot \vec{\nabla}_{\vec{q}} \delta^d(\vec{q}), \quad (\text{C11})$$

$$\overline{\overline{F}}'(\vec{q}, t_1) = e^{i\vec{v} \cdot \vec{q}t} \overline{\overline{F}}(\vec{q}, t_1). \quad (\text{C12})$$

Thus we have the identity

$$\frac{\delta\Gamma}{\delta\vec{v}} = 0 = \int d^d\vec{q}dt_1 \left\{ i \left[\vec{q}t_1\overline{F}(\vec{q}, t_1) - \kappa\delta^d(\vec{q})\vec{\nabla}_{\vec{q}} \right] \frac{\delta\Gamma}{\delta\overline{F}(\vec{q}, t_1)} + i\vec{q}t_1\overline{\overline{F}}(\vec{q}, t_1) \frac{\delta\Gamma}{\delta\overline{\overline{F}}(\vec{q}, t_1)} \right\}, \quad (\text{C13})$$

where Eqs. (C11) and (C12) have been used to obtain the variations of \overline{F} and $\overline{\overline{F}}$ with respect to \vec{v} . Taking functional derivatives of Eq. (C13) with respect to $\overline{\overline{F}}(\vec{k}, t)$ and $\overline{F}(\vec{k} - \vec{q}, t_2)$, then taking the limit $\overline{\overline{F}}, \overline{F} \rightarrow 0$, we obtain the following Ward identity in Fourier space,

$$\kappa\vec{\nabla}_{\vec{q}} \int dt_1 \widehat{\Gamma}_{1,2}(\vec{q}, t - t_1; \vec{k} - \vec{q}, t - t_2)|_{\vec{q} \rightarrow 0} = \vec{k}(t - t_2) \widehat{\Gamma}_{1,1}(\vec{k}, t - t_2), \quad (\text{C14})$$

where the definition

$$\begin{aligned} & \widehat{\Gamma}_{1,n}(\vec{q}_1, t - t_1; \dots; \vec{q}_n, t - t_n) (2\pi)^d \delta^d(\vec{q}_1 + \dots + \vec{q}_n + \vec{k}) \\ & \equiv \int d^d\vec{x} d^d\vec{x}_1 \dots d^d\vec{x}_n e^{i\vec{k}\vec{x} + i\vec{q}_1\vec{x}_1 + \dots + i\vec{q}_n\vec{x}_n} \frac{\delta^{(1+n)}\Gamma[\overline{\overline{F}}, \overline{F}]}{\delta\overline{\overline{F}}(\vec{x}, t) \delta\overline{F}(\vec{x}_1, t_1) \dots \delta\overline{F}(\vec{x}_n, t_n)} \end{aligned}$$

is used. It is more convenient to write Eq. (C14) in frequency space. With

$$\begin{aligned} & \widehat{\widehat{\Gamma}}_{1,n}(\vec{q}_1, \omega_1; \dots; \vec{q}_n, \omega_n) 2\pi\delta(\omega_1 + \dots + \omega_n + \omega) \\ & \equiv \int dt dt_1 \dots dt_n e^{-i\omega t - i\mu_1 t_1 - \dots - i\mu_n t_n} \widehat{\Gamma}_{1,n}(\vec{q}_1, t - t_1; \dots; \vec{q}_n, t - t_n), \end{aligned}$$

Eq. (C14) becomes

$$\kappa\vec{\nabla}_{\vec{q}} \widehat{\widehat{\Gamma}}_{1,2}(\vec{q}, \mu; \vec{k} - \vec{q}, \omega - \mu)|_{\vec{q}, \mu \rightarrow 0} = -i\vec{k} \frac{\partial}{\partial\omega} \widehat{\widehat{\Gamma}}_{1,1}(\vec{k}, \omega). \quad (\text{C15})$$

From Eq. (A15), we have

$$\widehat{\widehat{\Gamma}}_{1,1}(\vec{k}, \omega) = \widehat{\widehat{G}}^{-1}(\vec{k}, \omega), \quad (\text{C16})$$

where

$$\widehat{\widehat{G}}(\vec{k}, \omega) = \int dt \widehat{g}(qt^\zeta) e^{-i\omega t}. \quad (\text{C17})$$

In the simplest case where there is no disorder, we have

$$\widehat{\widehat{\Gamma}}_{1,1}^{(0)}(\vec{k}, \omega) = \frac{T}{2\kappa} k^2 - i\omega. \quad (\text{C18})$$

The Ward identity then reads

$$\kappa \vec{\nabla}_{\vec{q}} \widehat{\Gamma}_{1,2}^{(0)}(\vec{q}, \mu; \vec{k} - \vec{q}, \omega - \mu)|_{\vec{q}, \mu \rightarrow 0} = -\vec{k}, \quad (\text{C19})$$

yielding a “bare” three-point vertex

$$\widehat{\Gamma}_{1,2}^{(0)}(\vec{k}_1, \omega_1; \vec{k}_2, \omega_2) = -\frac{1}{\kappa} \vec{k}_1 \cdot \vec{k}_2, \quad (\text{C20})$$

since $\widehat{\Gamma}_{1,2}$ must be symmetric in \vec{k}_1 and \vec{k}_2 . This vertex is exactly Eq. (B11), which has been obtained directly from the dynamic functional $S[\widetilde{F}, F]$ in Appendix B.

For the random problem at hand, the scaling form Eq. (2.9) or (3.9) for G implies that the two-point vertex must have the following form:

$$\widehat{\Gamma}_{1,1}(\vec{k}, \omega) = k^{1/\zeta} \widetilde{\Gamma}_{1,1}(\omega/k^{1/\zeta}), \quad (\text{C21})$$

where

$$\widetilde{\Gamma}_{1,1}(s) = \nu_1(s) - i s \nu_2(s), \quad (\text{C22})$$

with ν_1, ν_2 being real, *dimensionless* scaling functions. Since \widehat{g} is real, ν_1 and ν_2 must be even functions. Furthermore, $\int_0^\infty dt \widehat{g}(qt^\zeta) \sim q^{-1/\zeta}$ since \widehat{g} is rapidly decreasing for large argument. It then follows that

$$\lim_{s \rightarrow 0} \nu_1(s) = \text{const} \quad \text{and} \quad \lim_{s \rightarrow 0} s \nu_2(s) = 0. \quad (\text{C23})$$

The Ward identity (C15) now leads to the relation

$$\widehat{\Gamma}_{1,2}(\vec{q}, \mu; \vec{k} - \vec{q}, \omega - \mu)|_{\vec{q}, \mu \rightarrow 0} = -\frac{1}{\kappa} \vec{q} \cdot (\vec{k} - \vec{q}) \nu(\omega/k^{1/\zeta}), \quad (\text{C24})$$

where $\nu(s) = i \frac{\partial}{\partial s} \widetilde{\Gamma}_{1,1}(s)$ is another dimensionless (but complex) scaling function,

$$\nu(s) = \nu_2(s) + s \frac{d\nu_2}{ds} - i \frac{d\nu_1}{ds}. \quad (\text{C25})$$

The above limiting behavior of $\widehat{\Gamma}_{1,2}$ is as much as the Ward identity will directly yield. However, it does *suggest* a natural scaling form for the full spatial and temporal dependence of the vertex,

$$\widehat{\Gamma}_{1,2}(\vec{k}_1, \omega_1; \vec{k}_2, \omega_2) = -\frac{1}{\kappa} \vec{k}_1 \cdot \vec{k}_2 V(\omega_2/k_2^{1/\zeta}, k_1/k_2, \omega_1/\omega_2), \quad (\text{C26})$$

where V is another complex, *dimensionless* scaling function, with $V(s, 0, 0) = \nu(s)$.

The scaling form Eq. (C26) of the full vertex $\widehat{\Gamma}_{1,2}$, together with mild convergence conditions on V , imply that the *scaling* properties obtained from the full vertex is the same as that obtained from the bare vertex (C20). We now illustrate this by computing the tail of the droplet distribution, or equivalently the singularity in $\widehat{W}'(\vec{q}, \tau \rightarrow \infty)$, using the full vertex.

In the limit $\tau \rightarrow \infty$, it is convenient to write Eq. (3.10) in frequency space,

$$\begin{aligned} \widehat{W}'(\vec{q}, t \rightarrow \infty) &= -T \int_{-\infty}^{\infty} \frac{d\omega}{2\pi} \widehat{\Gamma}_{1,2}(\vec{q}, \omega; -\vec{q}, -\omega) \widehat{G}(\vec{q}, \omega) \widehat{G}(-\vec{q}, -\omega) \\ &= -\frac{T}{\kappa} q^{2-1/\zeta} I, \end{aligned} \quad (\text{C27})$$

with

$$I = \int_{-\infty}^{\infty} \frac{ds}{2\pi} \frac{V(s, 1, 1)}{\nu_1^2(s) + s^2 \nu_2^2(s)}, \quad (\text{C28})$$

where we used Eqs. (C22) and (C26). The scaling form Eq. (3.15) is valid as long as the integral I converges. In Sec.III.A, we used the “bare” Γ ’s corresponding to $V = \nu_1 = \nu_2 = 1$. This gives the result $I = 1/2$. In general, we see that, given the properties of ν_1 and ν_2 in Eq. (C23), the integral converges if

$$V(s \rightarrow 0, 1, 1) < s^{-1} \quad \text{and} \quad V(s \rightarrow \infty, 1, 1) < s \nu_2^2(s). \quad (\text{C29})$$

Unfortunately, $V(s, 1, 1)$ is not directly obtainable from the Ward identity, which only gives $V(s, 0, 0)$. However, we do not expect $V(s, k_1/k_2, \omega_1/\omega_2)$ to depend strongly on the ratio k_1/k_2 and ω_1/ω_2 in the region $0 \leq k_1/k_2 \leq 1$ and $0 \leq \omega_1/\omega_2 \leq 1$. If we use $V(s, 0, 0) = \nu(s)$ for $V(s, 1, 1)$ with $\nu(s)$ given by Eq. (C25), then the convergence conditions (C29) are always satisfied given the properties of ν_1 and ν_2 in Eq. (C23). It is thus very reasonable to expect that (C29) are also satisfied by $V(s, 1, 1)$ itself, which then leads to the scaling result Eq. (3.15) for $\widehat{W}'(\vec{q}, \tau)$, with $\widehat{w}(s \rightarrow \infty) = I$.

Finally we note that although the scaling form (C26) for the vertex and the convergence conditions (C29) have not been derived from first principles, they are very plausible if an underlying renormalization group exists. This is especially true in 1+1 dimensions, where the strong coupling fixed point of the noisy-Burgers' equation can be described perturbatively via a $d = 2 - \epsilon$ renormalization-group expansion of the anisotropic driven diffusion equation (B4) in $d + 1$ dimensions as explained in Appendix B. The vertex function $\widehat{\Gamma}_{1,2}$ can be computed explicitly in the $2 - \epsilon$ expansion, and is indeed described by the scaling form Eq. (C26). Away from 1+1 dimensions for the noisy-Burgers' equation, a perturbative renormalization scheme is not known. However none of the known results give any indication of the break down of simple scaling. Thus we expect that the hypothesized scaling form (C26) for $\widehat{\Gamma}_{1,2}$ is valid in all dimensions for the Burgers' equation and therefore also for the directed polymer.

REFERENCES

- * Present address: School of Natural Sciences, Institute for Advanced Study, Princeton, NJ 08540; on leave from: Department of Physics, S.U.N.Y., Stony Brook, NY.
- [1] D. A. Huse and C. L. Henley, Phys. Rev. Lett. **54**, 2708, (1985).
- [2] D. A. Huse, C. L. Henley, and D. S. Fisher, Phys. Rev. Lett. **55**, 2924 (1985).
- [3] L. Ioffe and V. M. Vinokur, J. Phys. **C 20**, 6149, (1987).
- [4] M. Kardar and Y.-C. Zhang, Phys. Rev. Lett. **58**, 2087 (1987).
- [5] A. J. McKane and M. A. Moore, Phys. Rev. Lett. **60**, 527 (1988).
- [6] Y. Imry and S. K. Ma, Phys. Rev. Lett. **35**, 1399 (1976).
- [7] D. S. Fisher, Phys. Rev. Lett. **56** 1964 (1986).
- [8] M. V. Feigel'man, V. B. Geshkenbein, A. I. Larkin, and V. M. Vinokur, Phys. Rev. Lett. **63**, 2303 (1989).
- [9] J. P. Bouchaud, M. Mézard, J. Yedidia, Phys. Rev. Lett. **67**, 3840 (1991); Phys. Rev. **B 46**, 14686 (1992).
- [10] For a review, see K. Binder and A. P. Young, Rev. Mod. Phys. **58**, 801 (1986); and M. Mézard, G. Parisi, and M. A. Virasoro, *Spin Glass Theory and Beyond*, (World Scientific, Singapore, 1987).
- [11] D. Forster, D. R. Nelson, and M. J. Stephen, Phys. Rev. **A 16**, 732 (1977).
- [12] M. Kardar, G. Parisi, and Y. C. Zhang, Phys. Rev. Lett. **56**, 889 (1986); E. Medina, T. Hwa, M. Kardar, and Y. C. Zhang, Phys. Rev. **A 39**, 3053 (1989).
- [13] B. Derrida and H. Spohn, J. Stat. Phys. **51**, 817 (1988).
- [14] B. Derrida and R. B. Griffiths, Europhys. Lett. **8**, 111 (1989).

- [15] M. Kardar, Nucl. Phys. **B 290**, 582 (1987).
- [16] G. Parisi, J. Phys. (France) **51**, 1595 (1990).
- [17] M. Mézard and G. Parisi, J. Phys. I **1**, 809 (1991).
- [18] D. S. Fisher and D. A. Huse, Phys. Rev. **B 43**, 10728 (1991).
- [19] D. S. Fisher and D. A. Huse, Phys. Rev. **B 38**, 373 (1988); **B 38**, 386 (1988).
- [20] M. Mézard, J. Phys. (France) **51**, 1831 (1990).
- [21] J. M. Kim, M. A. Moore and A. J. Bray, Phys. Rev. **A 44**, 2345 (1991).
- [22] T. Halpin-Healy, Phys. Rev. **A 44**, R3415 (1991); J. Krug, P. Meakin, and T. Halpin-Healy, Phys. Rev. **A 45**, 638 (1992).
- [23] J. Z. Imbrie and T. Spencer, J. Stat. Phys. **52**, 609 (1988).
- [24] Y.-C. Zhang, Phys. Rev. Lett. **59**, 2125 (1987).
- [25] D. S. Fisher, unpublished. See, L. Balents and D. S. Fisher, Phys. Rev. B (to appear) for a discussion.
- [26] T. Hwa and E. Frey, Phys. Rev. **A 44**, R7873 (1991).
- [27] Alternatively, we can place two noninteracting polymers, $\vec{\xi}_a(z)$ and $\vec{\xi}_b(z)$, in the *same* random potential, both with the end $\vec{\xi}(t)$ fixed at \vec{x} . The disorder-averaged distribution $W_t(\vec{\Delta}, \tau)$ is just the average probability that the two polymers are separated by a distance $\vec{\Delta}$ at $z = t - \tau$, which only occurs when the sample has two nearly degenerate ground states that are located away from each other by a displacement $\vec{\Delta}$ at z .
- [28] The behavior of the off-diagonal response,

$$\chi_{ij}[\eta] = \frac{\partial}{\partial h_j} \langle \xi_i(0) \rangle_{\vec{h} \rightarrow 0},$$

with $i \neq j$ is also interesting and nontrivial. But we will not pursue this here in order to focus the study on the simplest rare fluctuations.

- [29] U. Schulz, J. Villain, E. Brézin, and H. Orland, *J. Stat. Phys.* **51**, 1 (1988).
- [30] For the directed polymers, the equilibrium properties can actually be studied numerically by the transfer matrix method which *enumerates* the “ground states” directly. This is what allows direct numerical studies of various distribution functions [21,22]. However this is a special feature of the *linear* nature of the polymer and is difficult to extend to higher dimensional systems such as an oriented manifold [7].
- [31] P. C. Martin, E. D. Siggia, and H. H. Rose, *Phys. Rev. A* **8**, 423 (1973).
- [32] C. A. Doty and K. M. Kosterlitz, preprint (1990).
- [33] T. Hwa and D. S. Fisher, to be published.
- [34] P. Bak, C. Tang, and K. Wiesenfeld, *Phys. Rev. Lett.* **59**, 381 (1987); *Phys. Rev. A* **38**, 364 (1988).
- [35] L. P. Kadanoff, S. R. Nagel, L. Wu, and S. M. Zhou, *Phys. Rev. A* **39**, 6524 (1989).
- [36] Z. Olami, H. J. S. Feder, and K. Christensen, *Phys. Rev. Lett.* **68**, 1244 (1992).
- [37] O. Narayan and D. S. Fisher, *Phys. Rev. B* (in press).
- [38] P. Le Doussal and T. Giarmachi, submitted to *Phys. Rev. Lett.*
- [39] Rare events are also uncovered in the replica-symmetric solution of the directed polymer in $1 + 1$ dimensions [16], where a free-energy functional of the type described in Appendices A and B is used.
- [40] Our analysis based on the “evolution” of the free energy for successively larger systems somewhat resembles the “cavity method” introduced in the study of mean-field spin glasses [10].
- [41] H. K. Janssen, *Z. Phys.* **B 23**, 377 (1976).
- [42] D. J. Amit, *Field Theory, the Renormalization Group, and Critical Phenomena*, (World

Scientific, Singapore, 1984).

- [43] For a review, see e.g., J. Krug and H. Spohn, in *Solids far from Equilibrium*, ed. C. Godreche (Cambridge University Press, 1991).
- [44] H. van Beijeren, R. Kutner, and H. Spohn, *Phys. Rev. Lett.* **54**, 2026 (1985).
- [45] H. K. Janssen and B. Schmittmann, *Z. Phys.* **B 63**, 517 (1986).
- [46] T. Hwa, *Phys. Rev. Lett.* **69**, 1552 (1992).
- [47] J. P. Bouchaud and M. Cates, *Phys. Rev.* **E 47**, R1455 (1993) and unpublished.
- [48] J. P. Doherty, M. A. Moore, J. M. Kim, A. J. Bray, to be published.

FIGURES

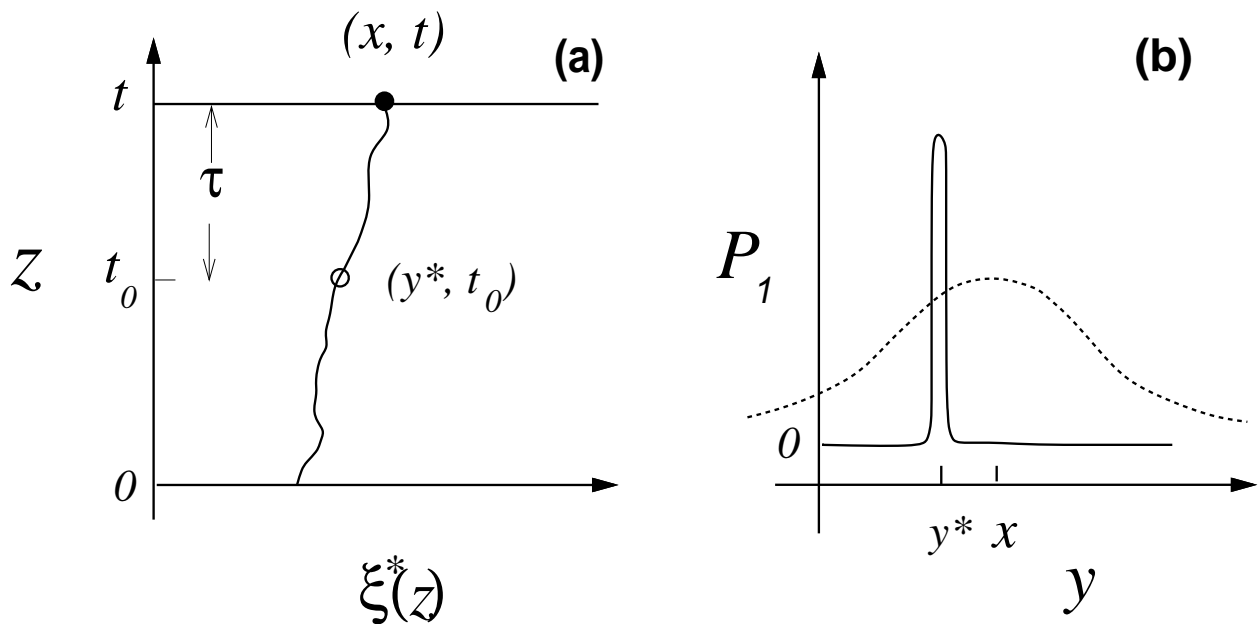


FIG. 1. (a) Schematic of the ground state $\xi^*(z)$ of a typical directed polymer with one end fixed at (\vec{x}, t) (the solid circle). The position of a segment at $z = t_0$ (open circle) is at $\xi^*(t_0) = \vec{y}^*$. (b) The one-point distribution function $P_1(\vec{y}, t_0|\vec{x}, t)$ as a function of \vec{y} . It is sharply peaked near some sample-specific \vec{y}^* with $|\vec{y}^* - \vec{x}| \sim \tau^\zeta$, where $\tau = t - t_0$. The dashed line indicates the disorder-averaged distribution function $G_t(\vec{x} - \vec{y}, \tau) = \bar{P}_1(\vec{y}, t_0|\vec{x}, t)$, which is centered about \vec{x} , with a width τ^ζ . This gives the distribution of \vec{y}^* from sample-to-sample.

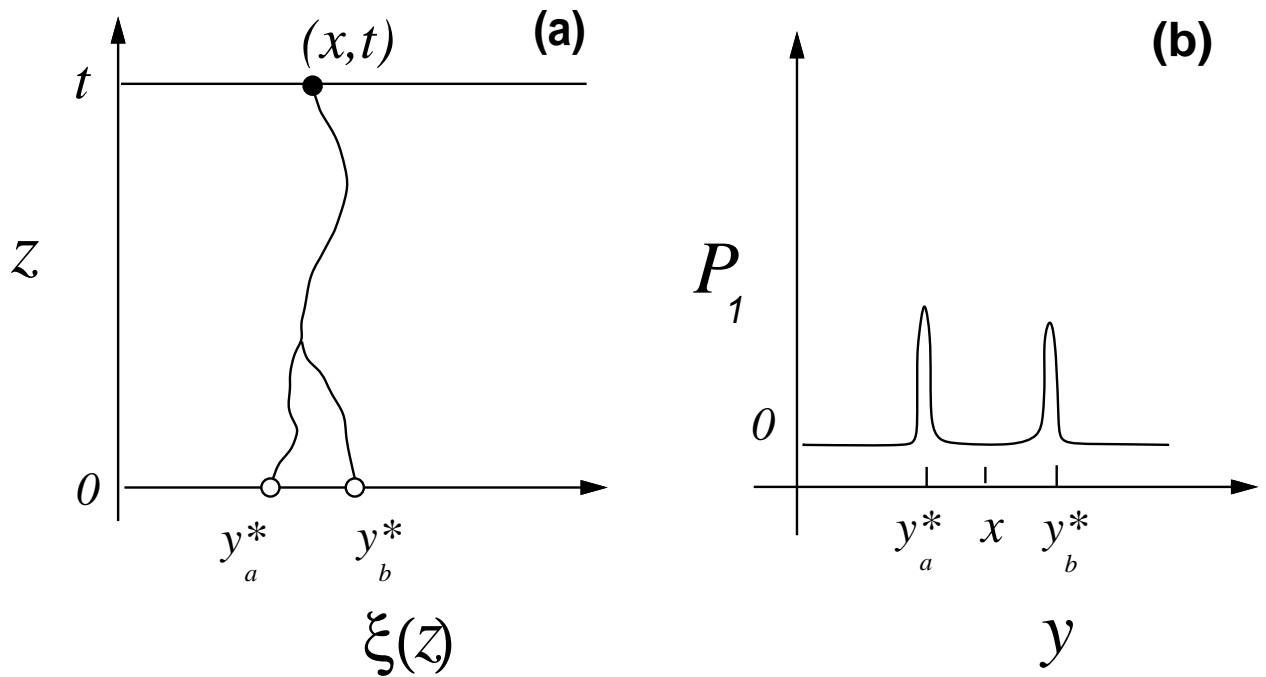


FIG. 2. (a) Behavior with a configuration of the random potential that gives rise to two almost-degenerate “ground states” $\vec{\xi}_a^*(z)$ and $\vec{\xi}_b^*(z)$ for a directed polymer with one end fixed at (\vec{x}, t) . The positions of the free ends of the two states are $\vec{\xi}_a^*(0) = \vec{y}_a^*$ and $\vec{\xi}_b^*(0) = \vec{y}_b^*$. (b) The end-point distribution function $P_1(\vec{y}, 0 | \vec{x}, t)$ for the sample in (a) displays two peaks at \vec{y}_a^* and \vec{y}_b^* .

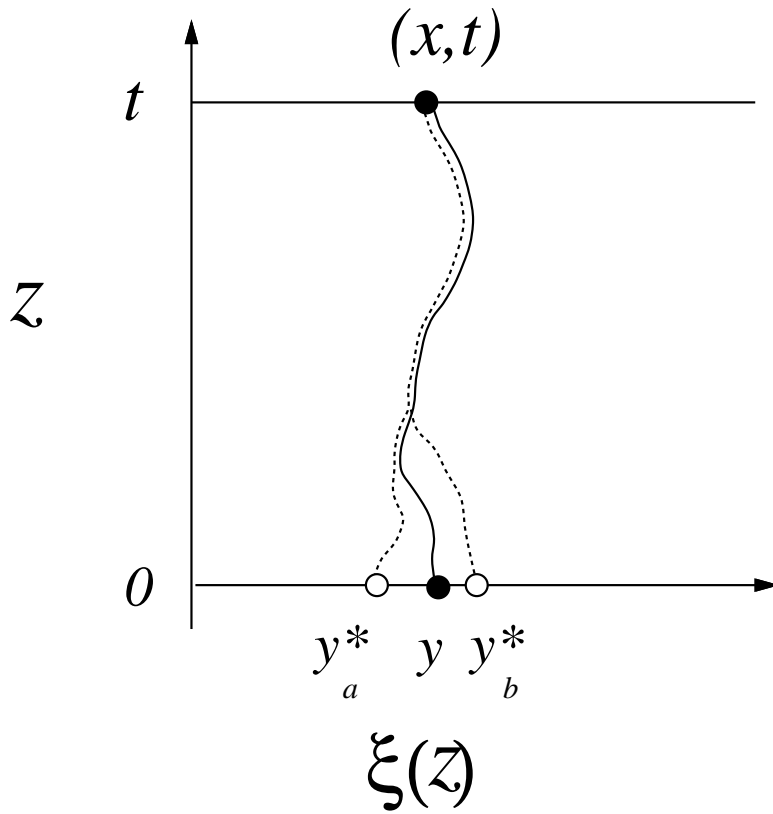


FIG. 3. The dotted lines are the degenerate ground states $\vec{\xi}_a^*(z)$ and $\vec{\xi}_b^*(z)$ shown in Fig. 2(a). The solid line is the optimal path with *both* ends fixed: $\vec{\xi}(t) = \vec{x}$ and $\vec{\xi}(0) = \vec{y}$, where \vec{y} is between \vec{y}_a^* and \vec{y}_b^* , which are separated by a distance of order Δ .

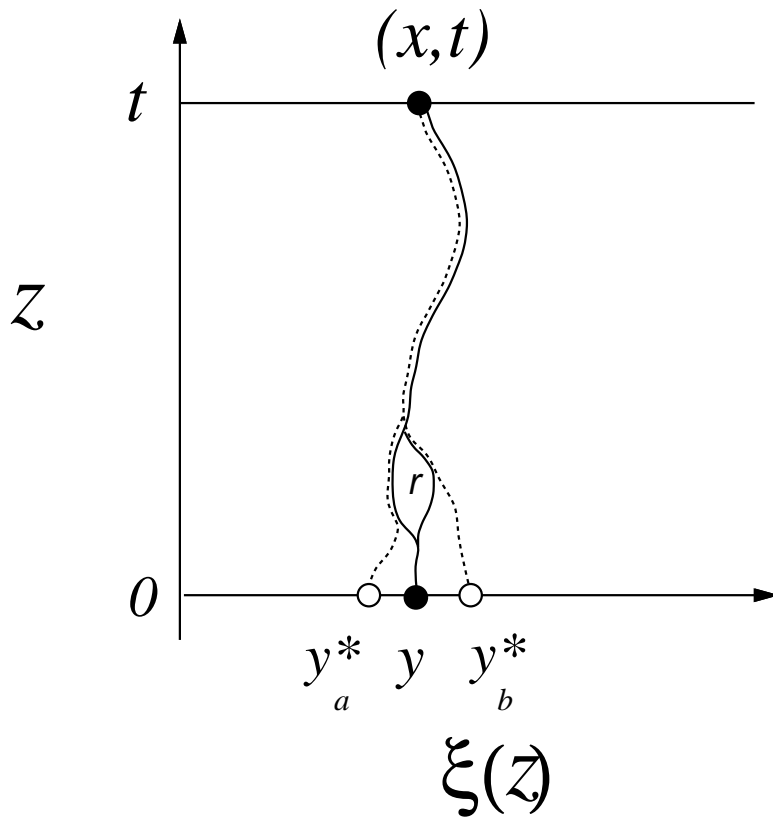


FIG. 4. The solid line illustrates a possible degenerate configuration of size r in the bulk for the optimal path shown in Fig. 3. Some energy barrier separates the two degenerate pieces of the optimal paths to \bar{y} . These will affect the energy barrier to move the polymer from between its almost-degenerate ground states ending at y_a^* and y_b^* .

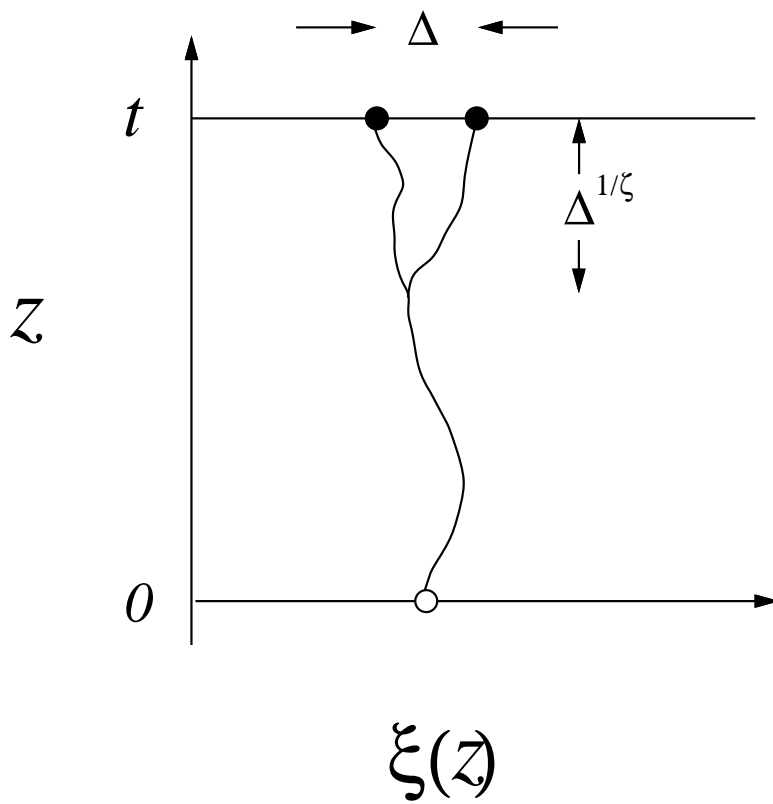


FIG. 5. Two polymers with ends fixed at a distance Δ apart typically merge at a distance $\Delta^{1/\zeta}$ from the fixed ends.

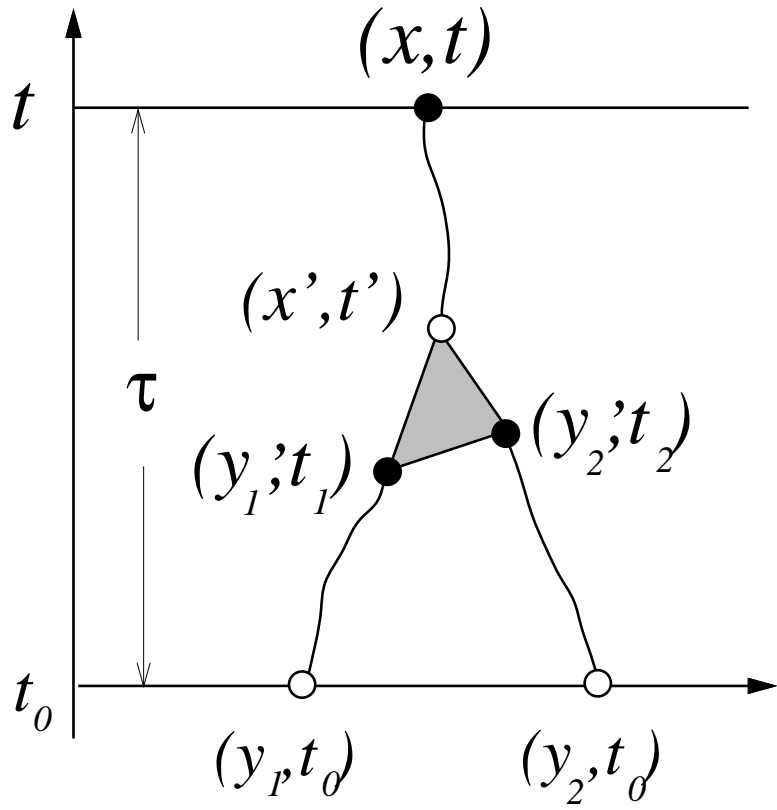


FIG. 6. The three-point function $G_{2,1}$ can be obtained as the convolution of three one-point functions G 's and a vertex function $\Gamma_{1,2}$ (the shaded triangle) which controls the branching process.

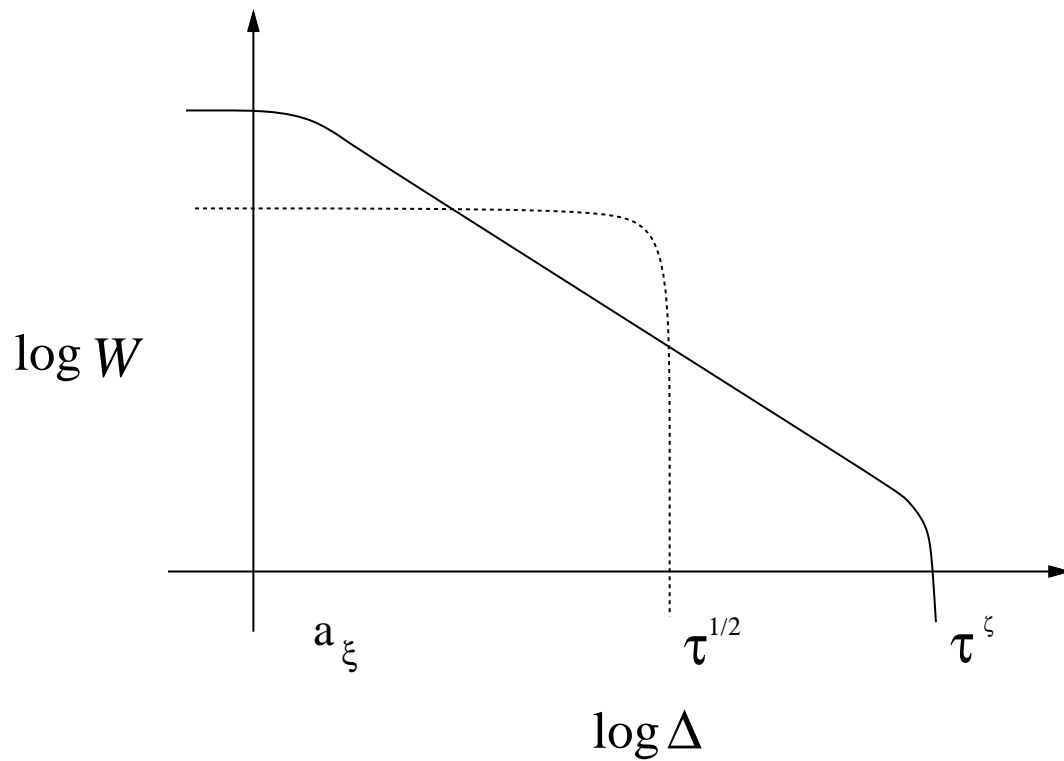


FIG. 7. The distribution function of the active droplet of size Δ , $W(\vec{\Delta}, \tau)$ (the solid line), is composed of two parts: A smooth piece for $\Delta \leq a_\xi(T)$, the small scale cutoff, and a long power-law tail extending to τ^ζ . The dashed line is the gaussian distribution $W^{(0)}(\vec{\Delta}, \tau)$ which describes the pure system (and the high temperature phase of the disordered system). It has a width of $O(\tau^{1/2})$.

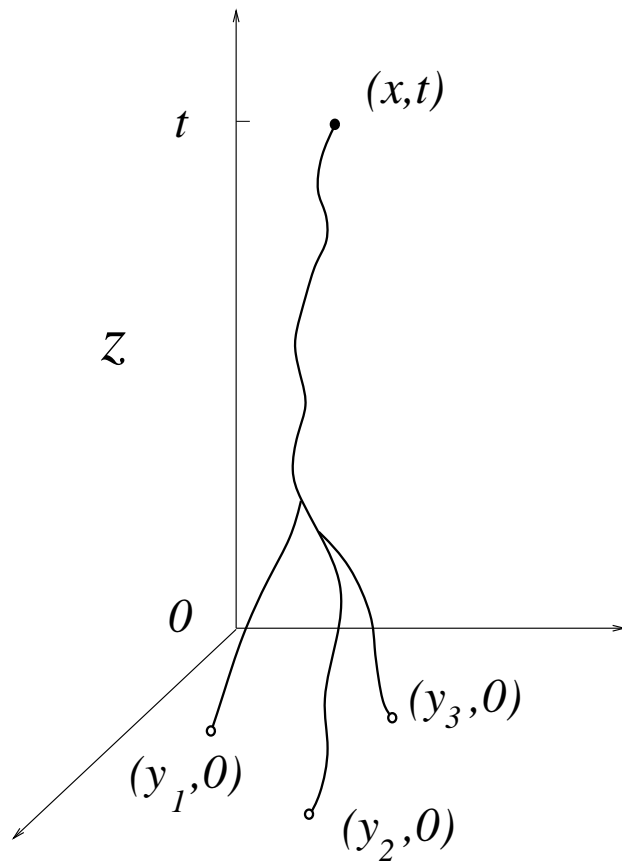


FIG. 8. A triply degenerate ground state configuration for a directed polymer in 2+1 dimensions, with the distance between each pair of end points being of order t^ζ for a polymer of length t .